Supporting Information

Fluorescent Probes for Sensitive and Selective Detection of pH Changes in Live Cells in Visible and Near-infrared Channels

Mingxi Fang,[a] Rashmi Adhikari,[a] Jianheng Bi,[a] Nethaniah Dorh,[a] Wafa Mazi,[a] Jianbo Wang,[a] Nathan Conner,[a] Jon Ainsley,[c] Tatyana G. Karabencheva-Christova,[a] Fen-Tair Luo,[b*] Ashutosh Tiwari,[a*] and Haiying Liu[a*]

[a]Department of Chemistry, Michigan Technological University, Houghton, MI 49931, E-mail: tiwari@mtu.edu; hyliu@mtu.edu

[b]Institute of Chemistry, Academia Sinica, Taipei, Taiwan 11529, Republic of China, E-mail: luoft@gate.sinica.edu.tw

[c]Department of Applied Sciences, Northumbria University , Newcastle upon Tyne NE1 8ST, UK

CONTENTS

Optical Measurement:

The UV-Vis absorption spectra of fluorescent probes **A**, **B, C, D** and **E** for pH dependency, selectivity, photostability and solvent effect measurements were collected in the range from 300 to 800 nm with increments of 1 nm. Their corresponding fluorescence spectra were collected at the excitation wavelength of 470 nm, 490 nm, and 580 nm for fluorescent probes **A**, **B**, **C, D** and **E** with increments of 1 nm, respectively. The excitation and emission slit widths were set up to 5 nm. The concentration of the dye in each sample is 5 μM. The quantum yields were calculated according to reference reported[1]. Fluorescence quantum yields were calculated by measuring fluorescence of a fluorophore of known quantum yield, which was Hunan dye dissolved in Ethyl Alcohol[2], with the same experimental parameters (excitation wavelength and slit width). Both samples and references were freshly prepared under identical conditions. The fluorescence quantum yields were calculated using the following equation:

$$\Phi_X = \Phi_{st}(Grad_X/Grad_{st})(\eta_X^2/\eta_{st}^2)$$

Where the subscripts '*st*' and '*X*' represent standard and testing sample, respectively, Φ stands for the fluorescence quantum yield, "*Grad*" is the gradient from the plot of integrated fluorescence intensity versus absorbance and *η* is the refractive index of the solvent.

Determination of pK_a by fluorometric titration

The constants K_a of fluorescent probes **A**, **B**, **C**, **D** and **E** related to spirolactam ring opening were determined by fluorometric titration as a function of pH in buffers with different pH values. The expression of the steady-state fluorescence intensity *F* as a function of the proton ion concentration has been extended for the case of a n: 1 complex between H^+ and a fluorescent probe, which is expressed by the equation below:[3]

$$F = \frac{F_{min}[H^+]^n + F_{max}K_a}{K_a + [H^+]^n}$$

F_{min} and F_{max} stand for the fluorescence intensities at maximal and minimal H^+ concentrations, respectively, and *n* is apparent stoichiometry of H^+ binding to the probe which causes the fluorescence change. Nonlinear fitting of equation expressed above to the fluorescence titration data recoded as a function of H^+ concentration with K_a and n as free adjustable parameters yields the estimated apparent constant of K_a.

^{1}H and ^{13}C NMR spectra of fluorescent probes A, B and C

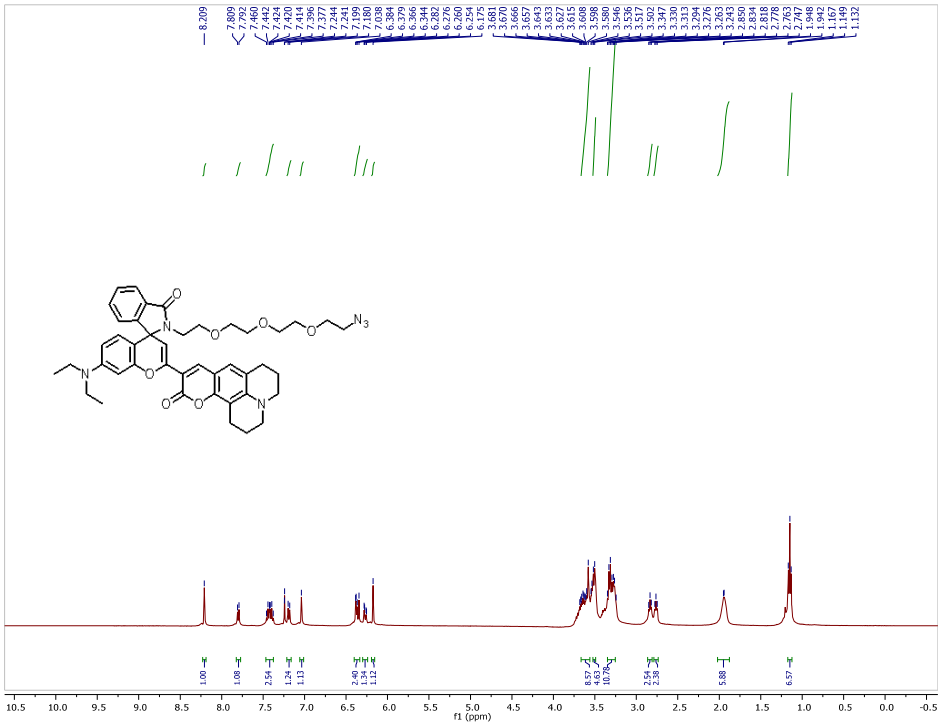

Figure S1. ^{1}H NMR spectrum of fluorescent probe **A** in $CDCl_3$ solution.

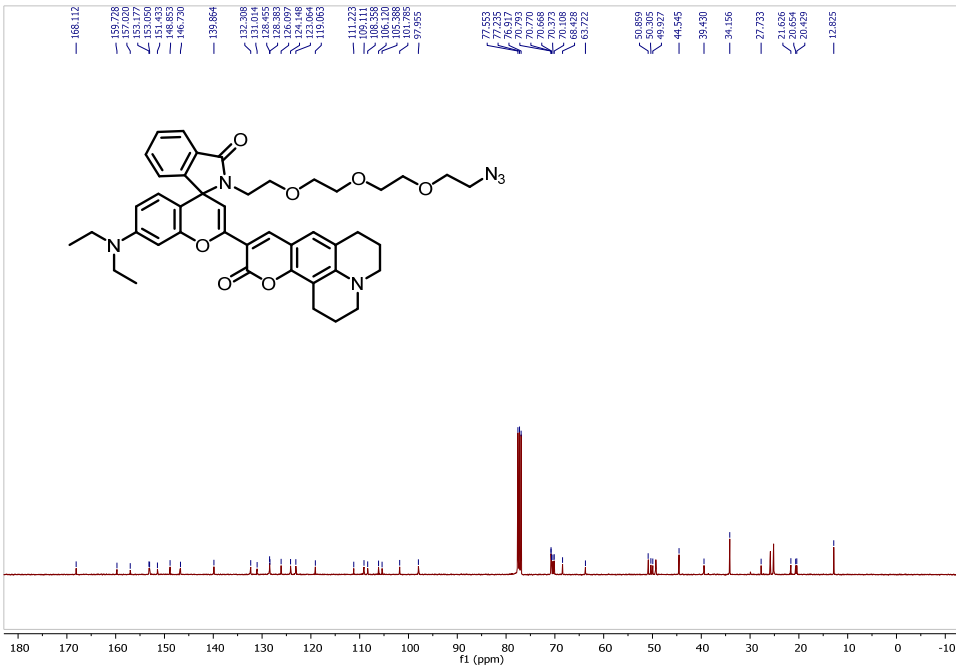

Figure S2. ^{13}C NMR spectrum of fluorescent probe **A** in $CDCl_3$

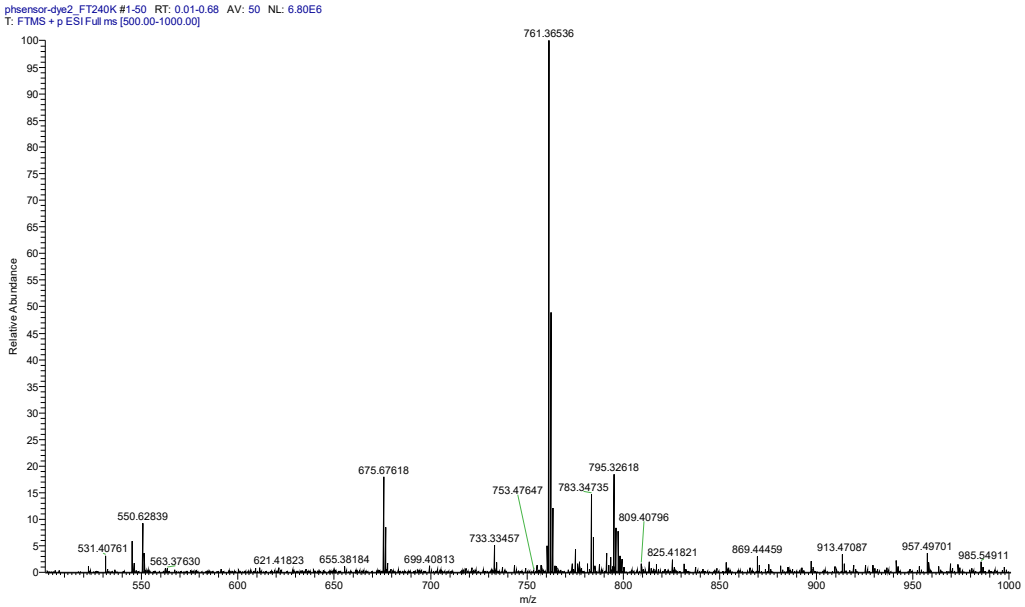

Figure S3. HRMS spectrum of fluorescent probe **A**.

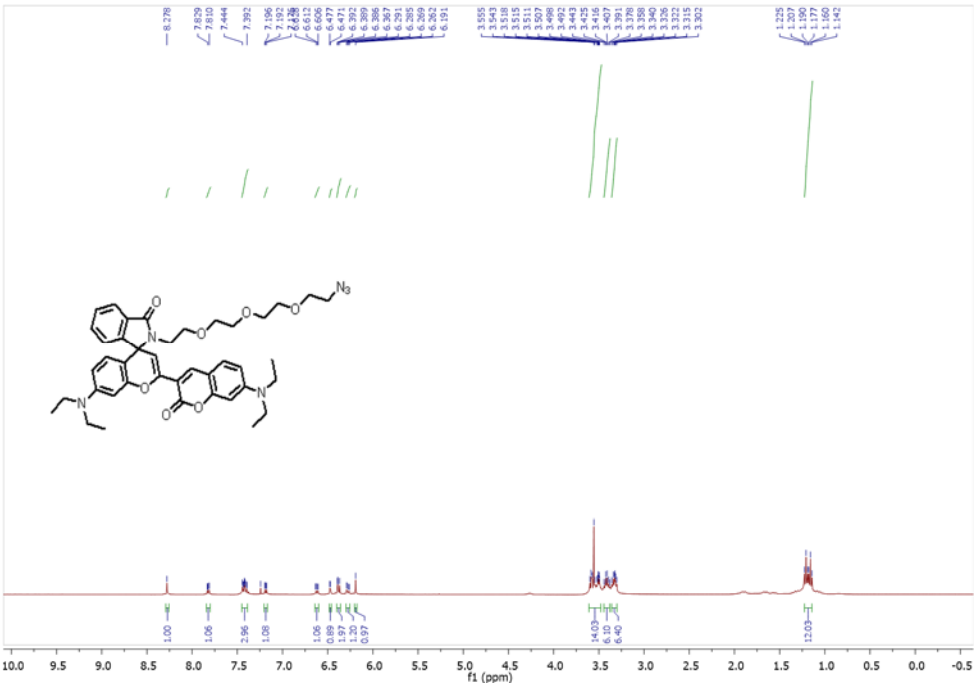

Figure S4. ^{1}H NMR spectrum of fluorescent probe **B** in $CDCl_3$ solution.

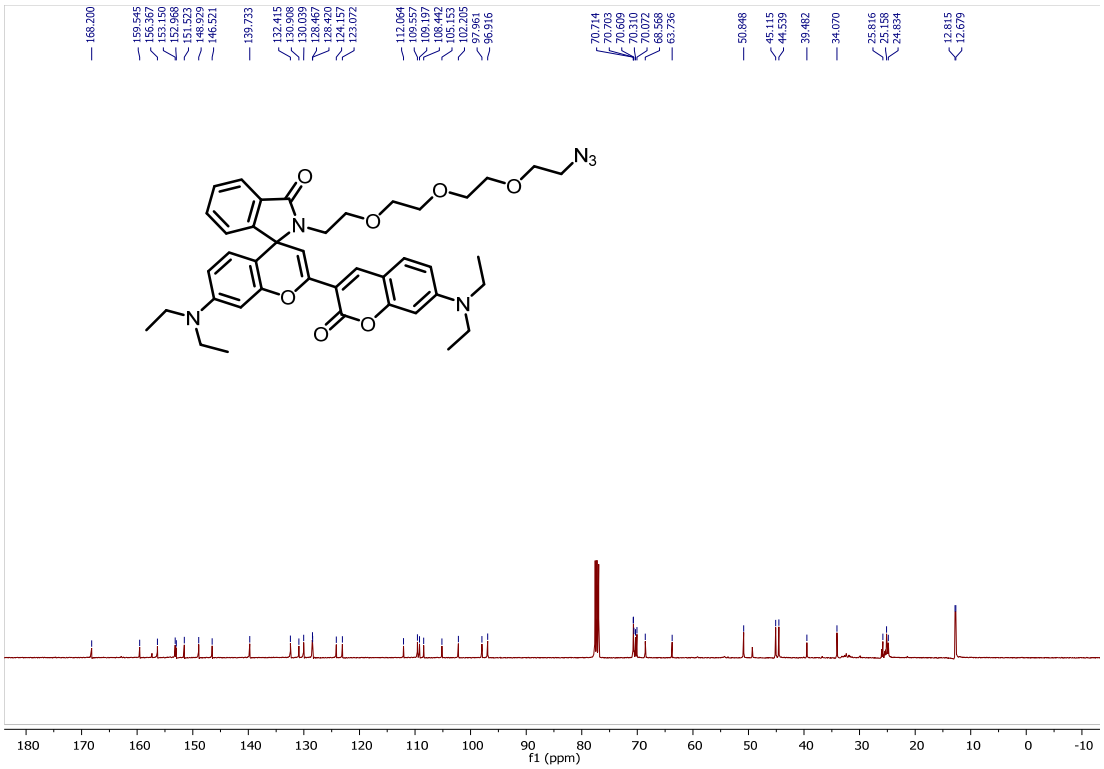

Figure S5. ^{13}C NMR spectrum of fluorescent probe **B** in $CDCl_3$ solution.

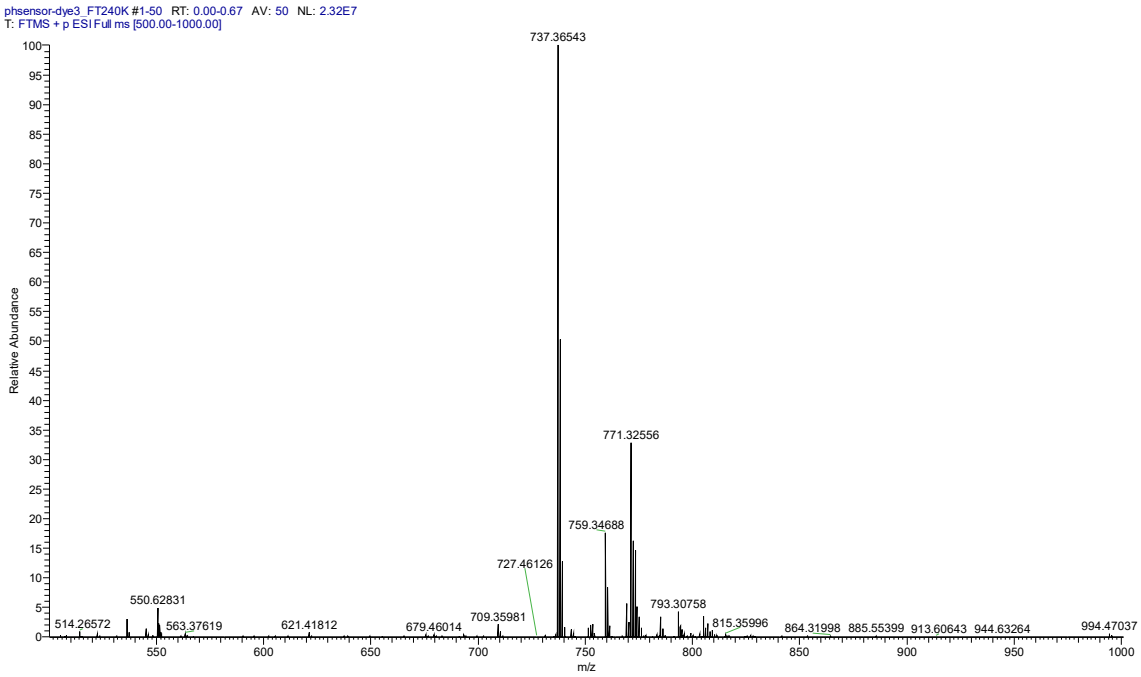

Figure S6. HRMS spectrum of fluorescent probe **B**.

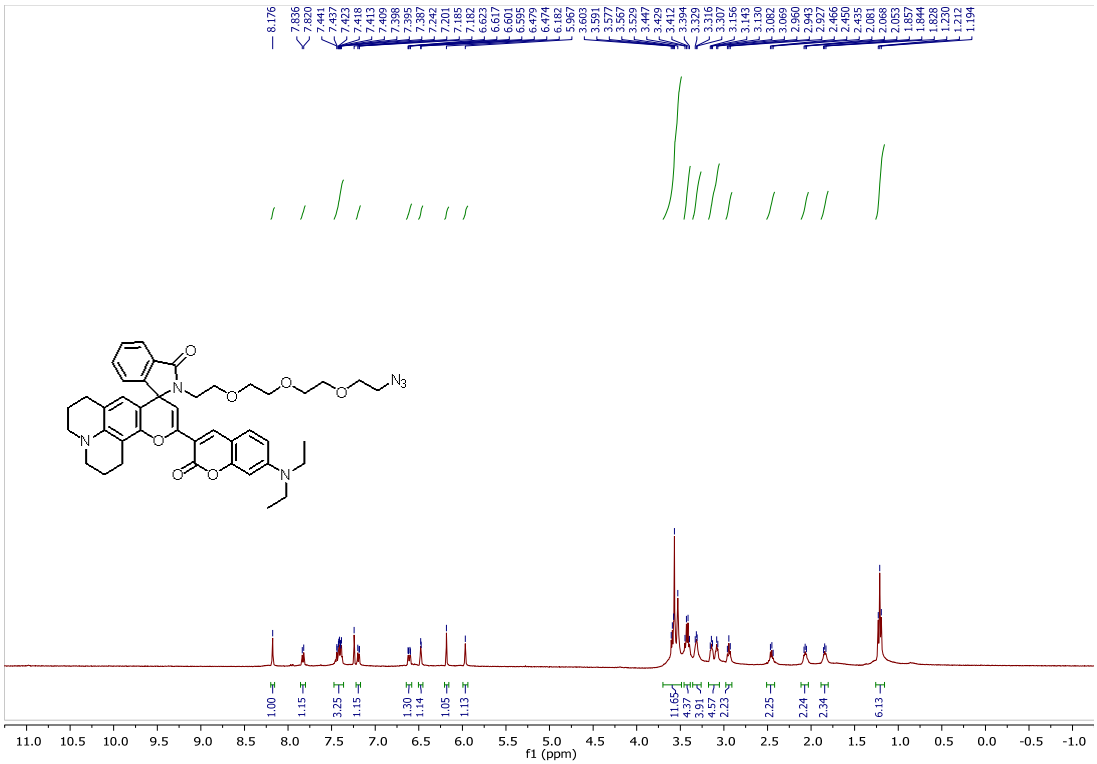

Figure S7. ^{1}H NMR spectrum of fluorescent probe **C** in $CDCl_3$ solution.

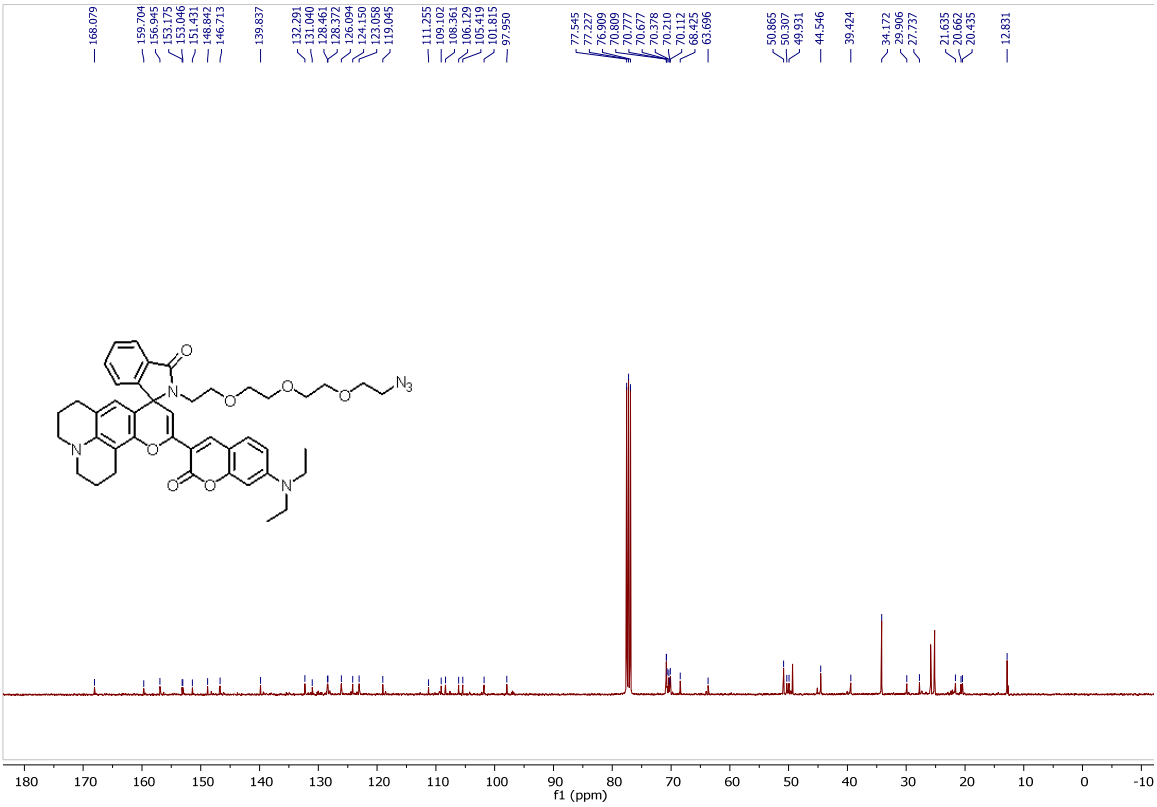

Figure S8. ^{13}C NMR spectrum of fluorescent probe **C** in $CDCl_3$ solution.

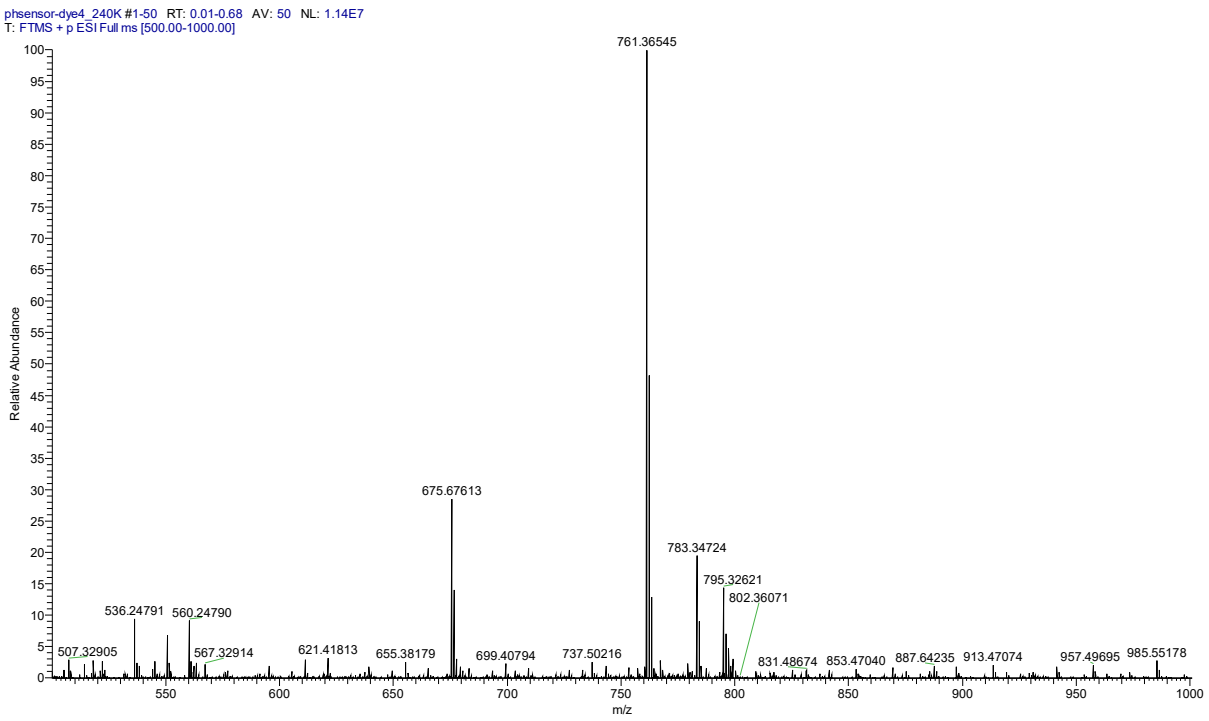

Figure S9. HRMS spectrum of fluorescent probe **C**.

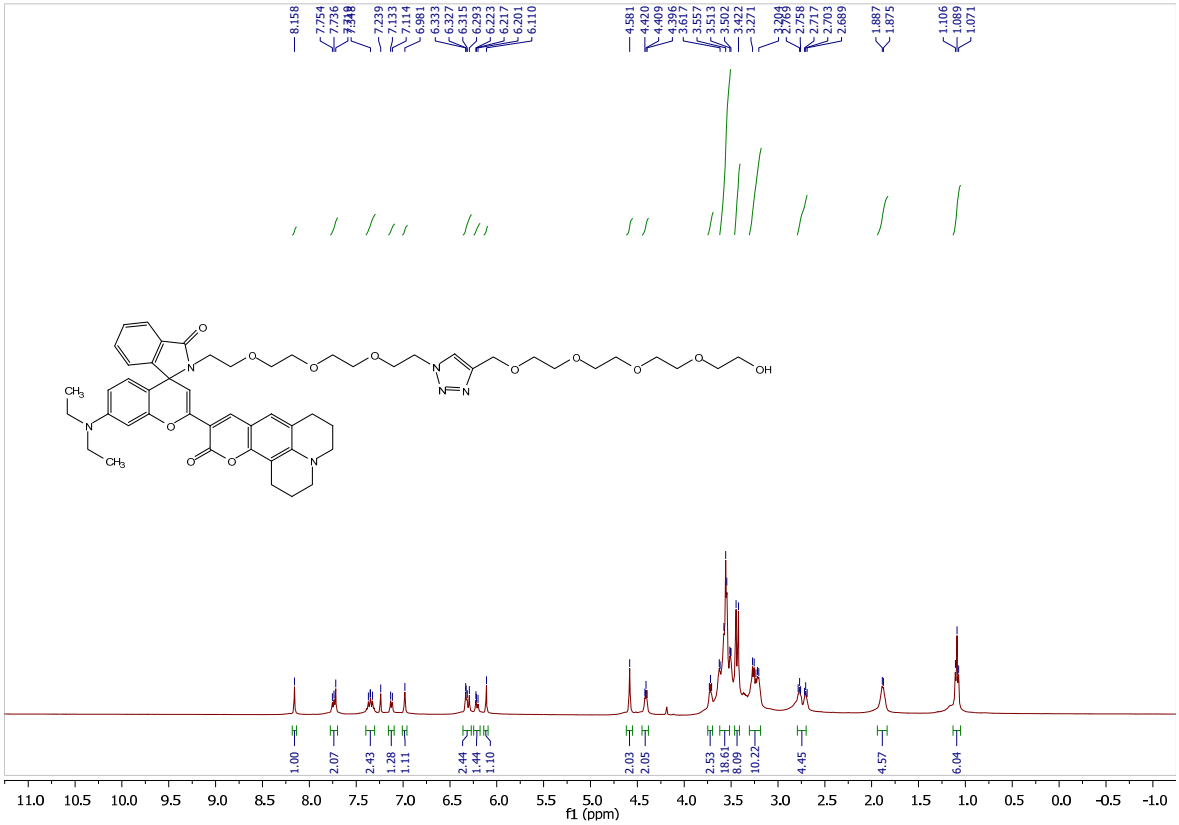

Figure S10. ^{1}H NMR spectrum of fluorescent probe **D** in $CDCl_3$ solution.

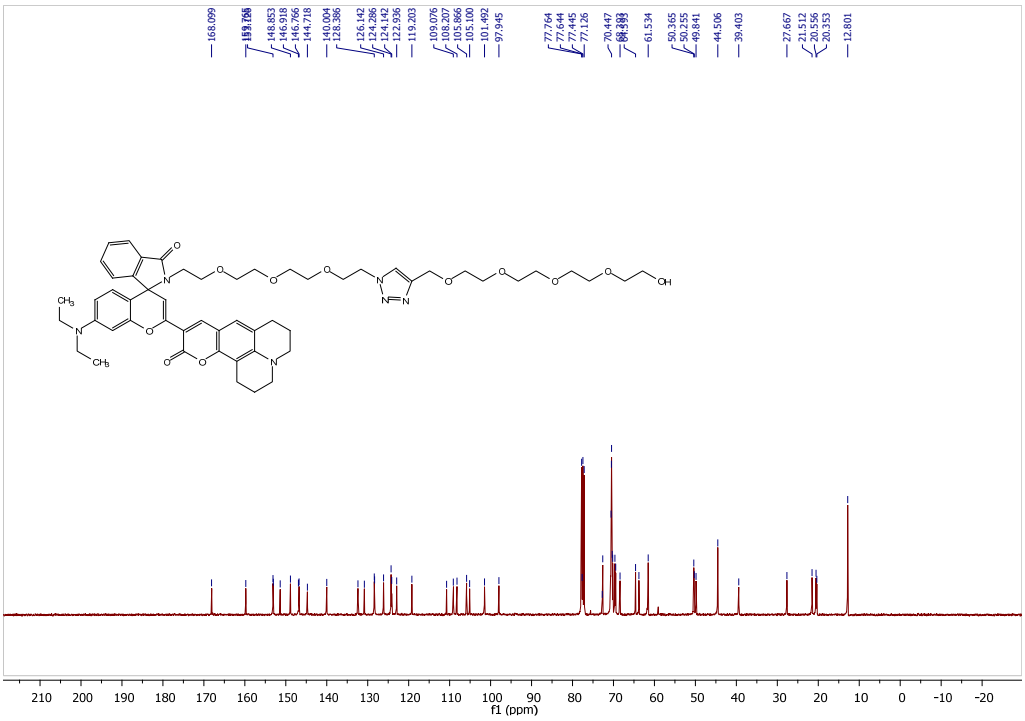

Figure S11. ^{13}C NMR spectrum of fluorescent probe **D** in $CDCl_3$ solution.

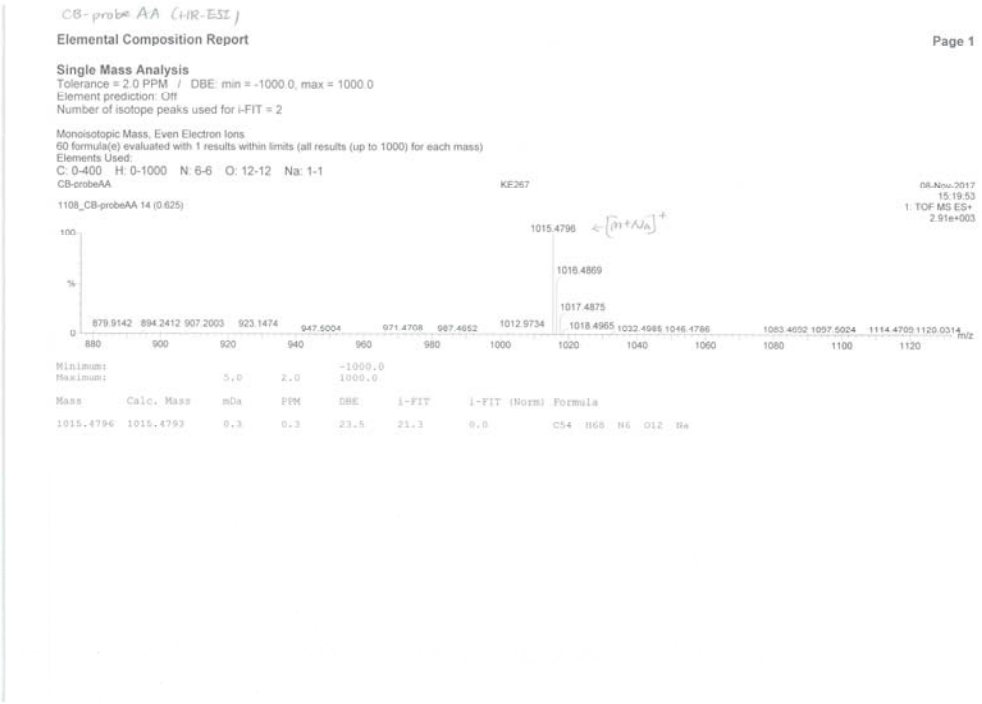

Figure S12. HRMS spectrum of fluorescent probe **D**.

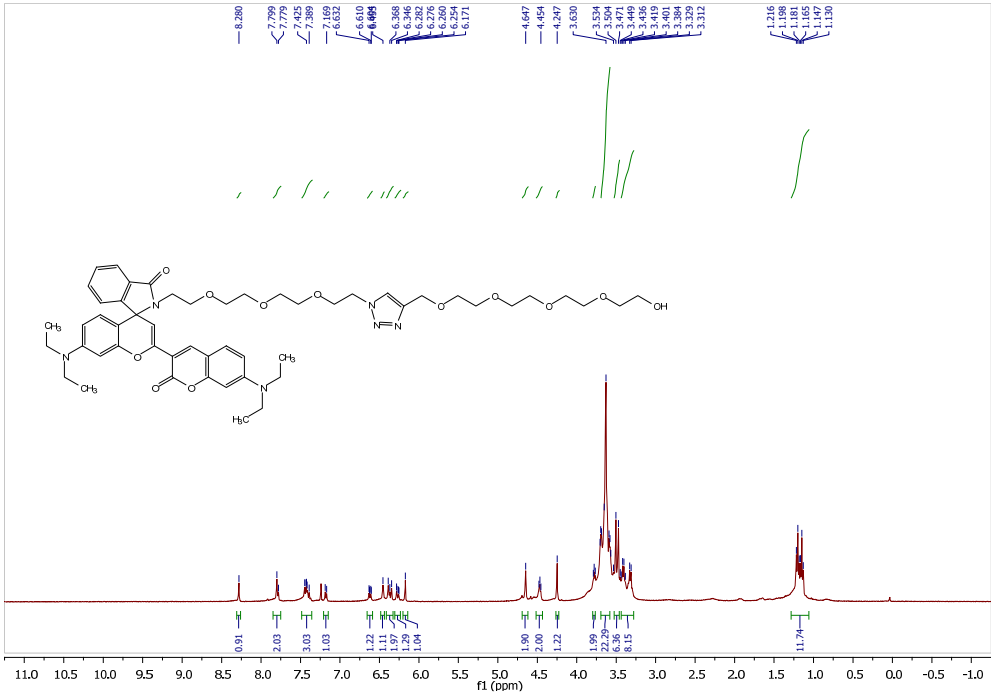

Figure S13. ^{1}H NMR spectrum of fluorescent probe **E** in $CDCl_3$ solution.

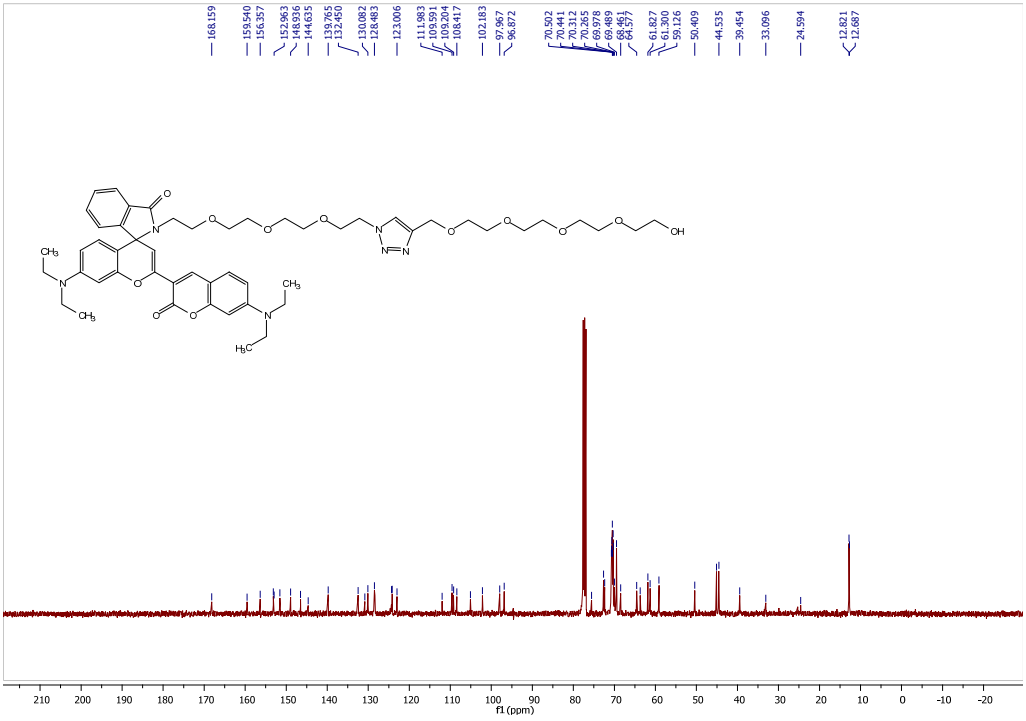

Figure S14. ^{13}C NMR spectrum of fluorescent probe **E** in $CDCl_3$ solution.

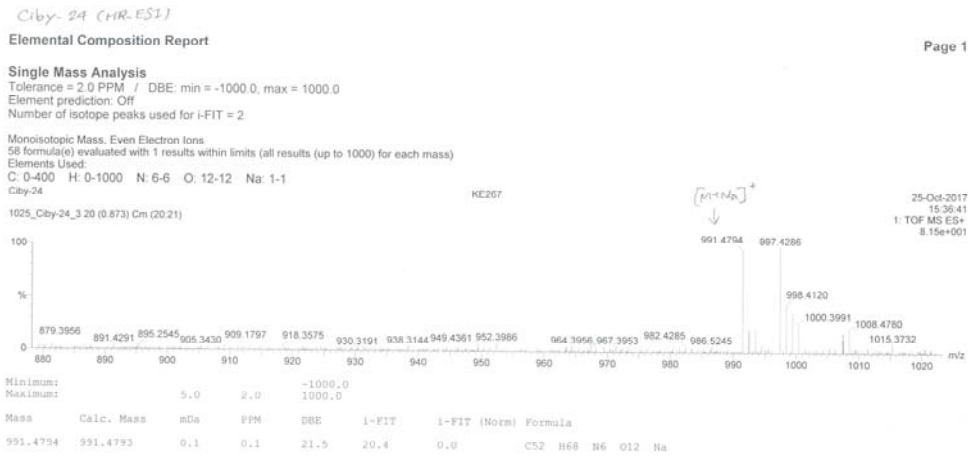

Figure S15. HRMS spectrum of fluorescent probe **E**.

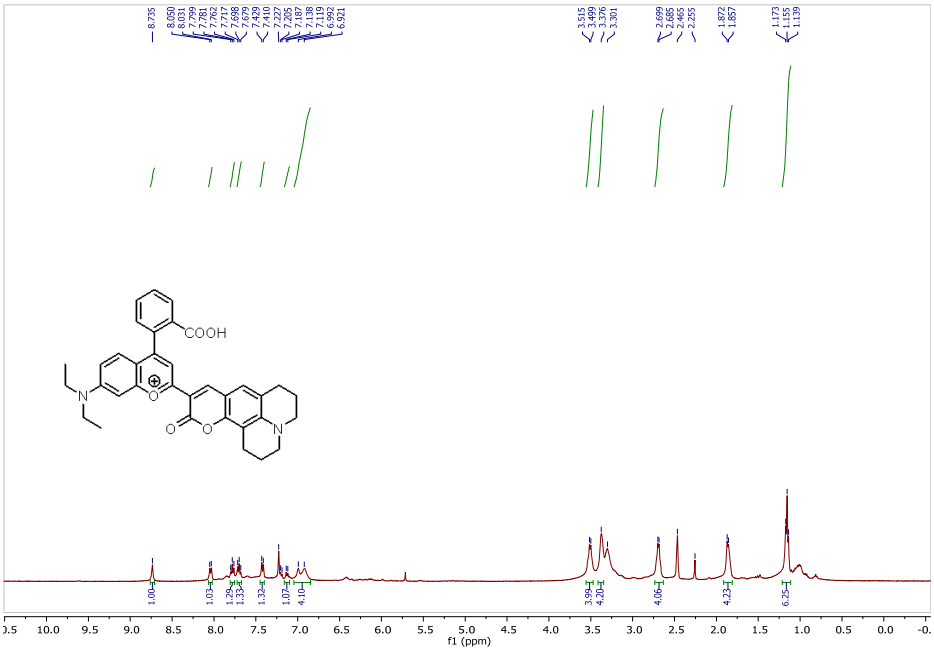

Figure S16. ^{1}H NMR spectrum of compound **3** in DMSO solution.

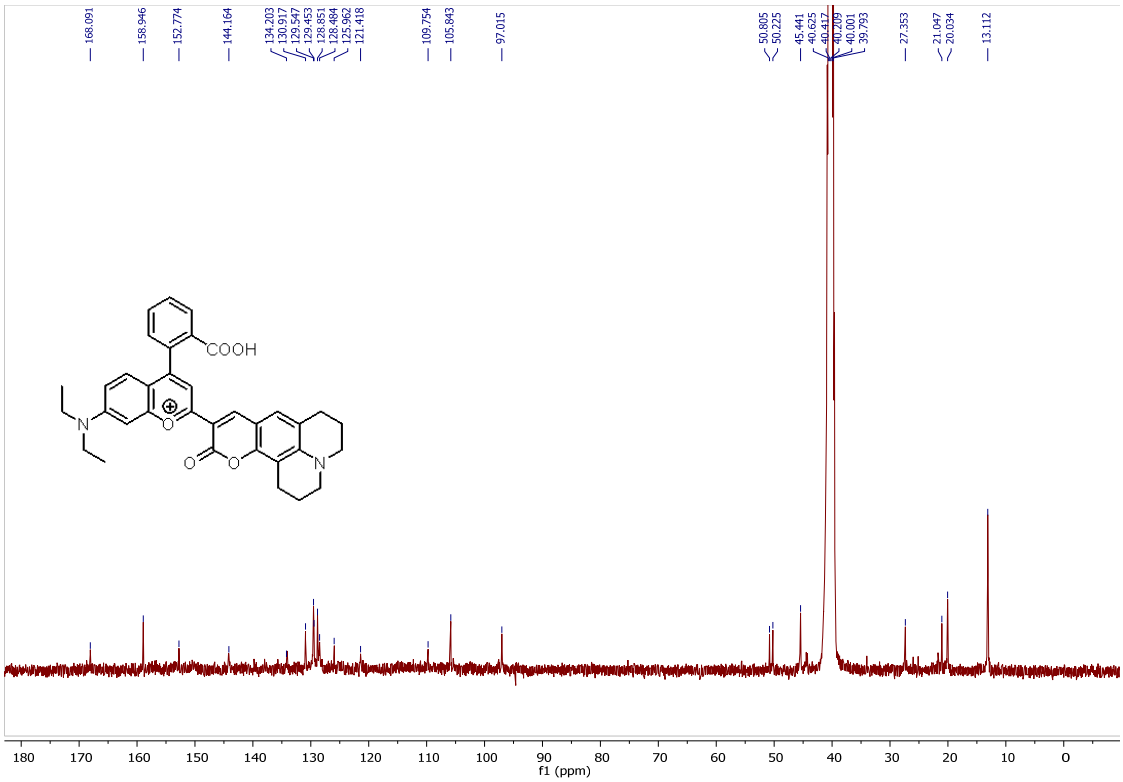

Figure S17. ^{13}C NMR spectrum of compound **3** in DMSO solution.

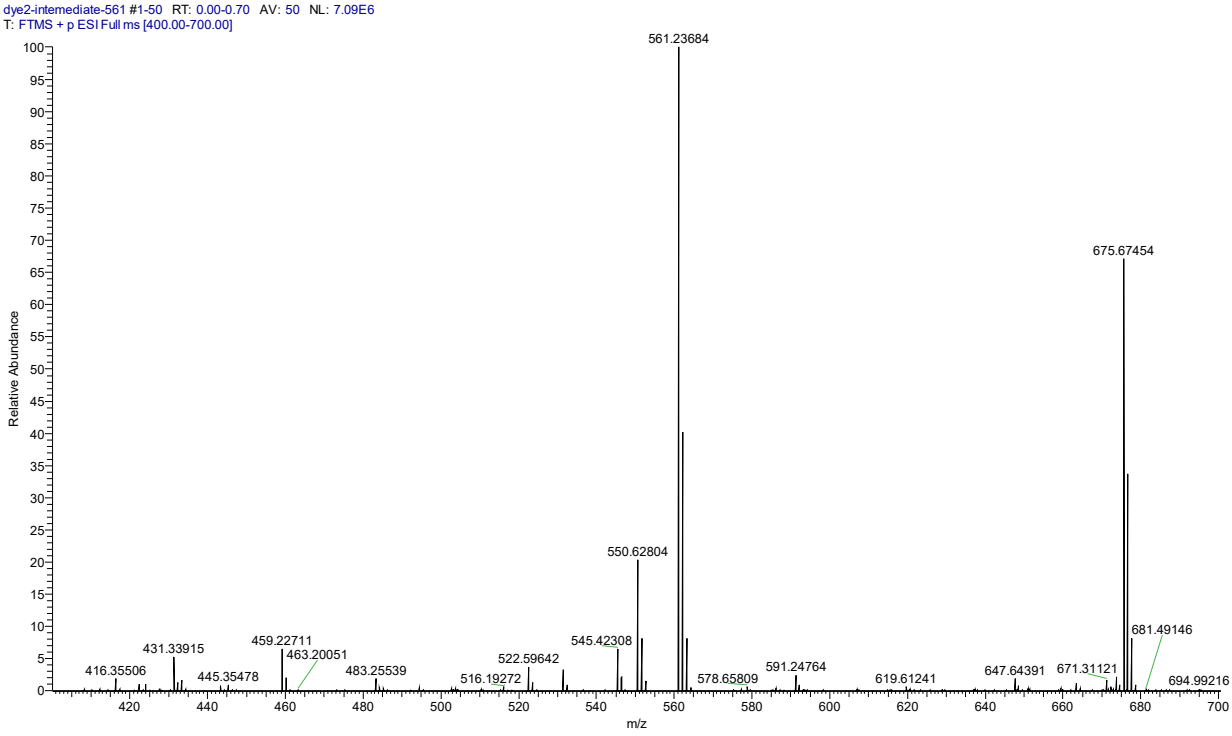

Figure S18. HRMS spectrum of compound **3**.

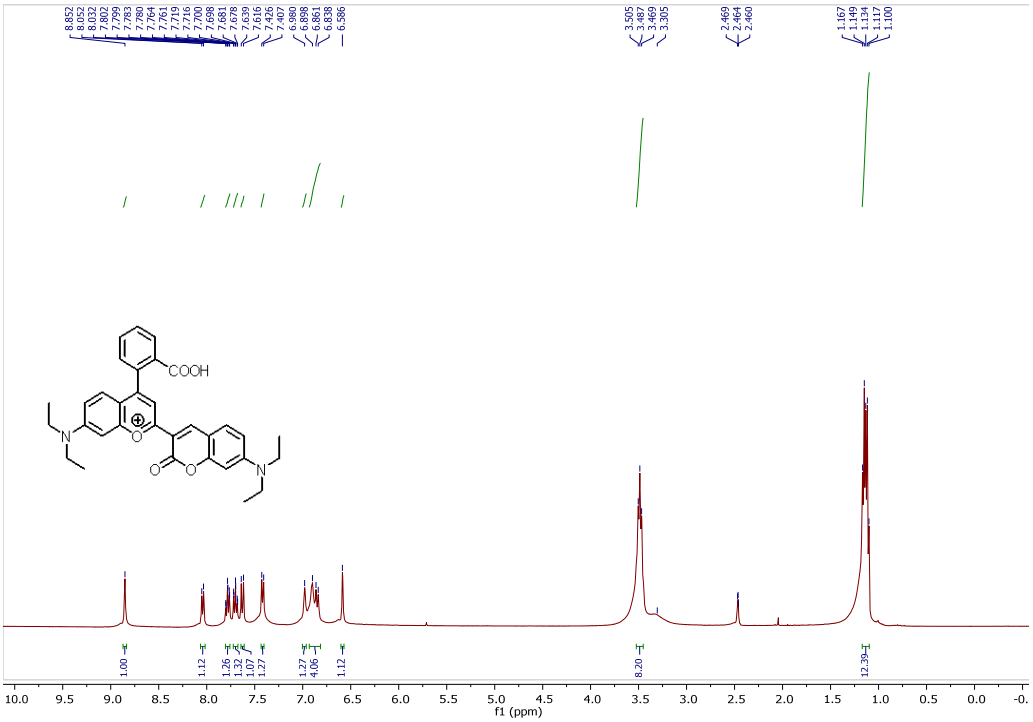

Figure S19. ^{1}H NMR spectrum of compound **6** in DMSO solution.

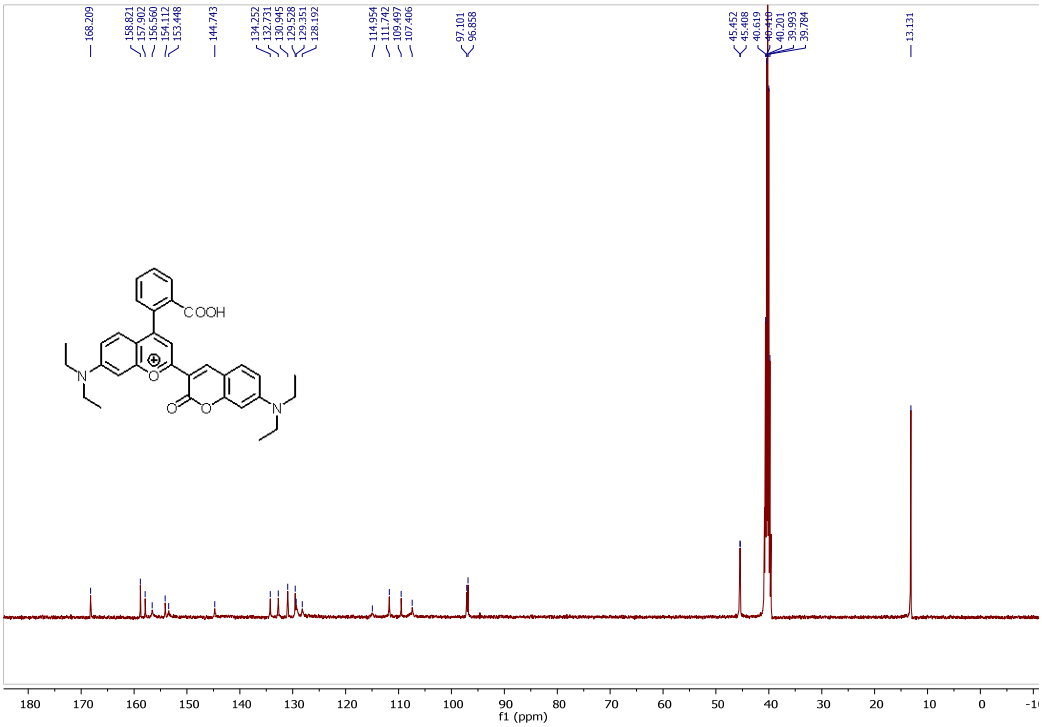

Figure S20. ^{13}C NMR spectrum of compound **6** in DMSO solution.

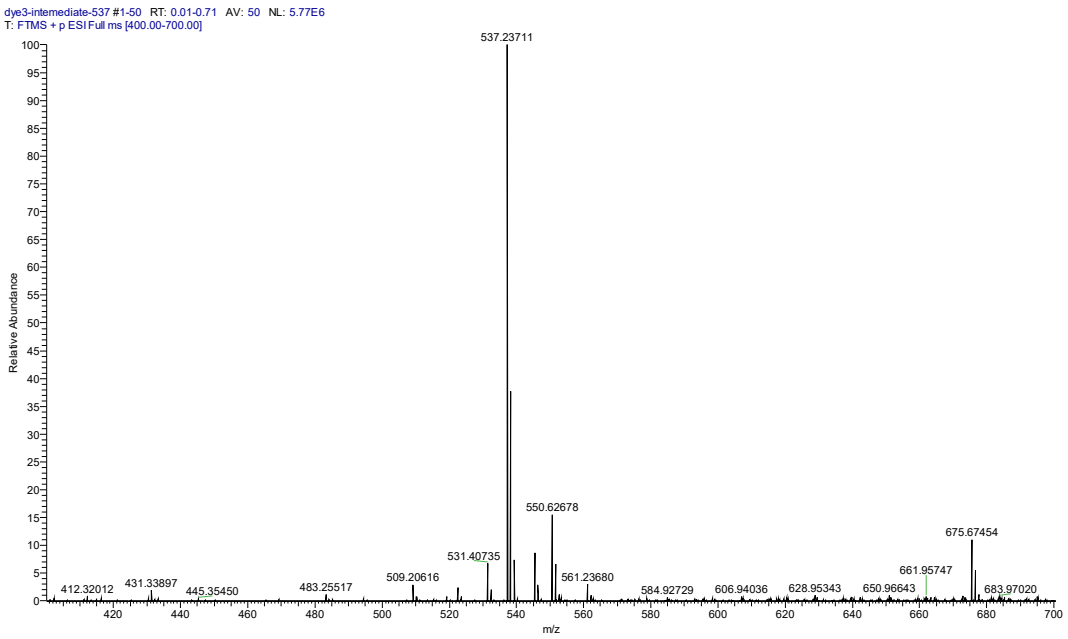

Figure S21. HRMS spectrum of compound **6**.

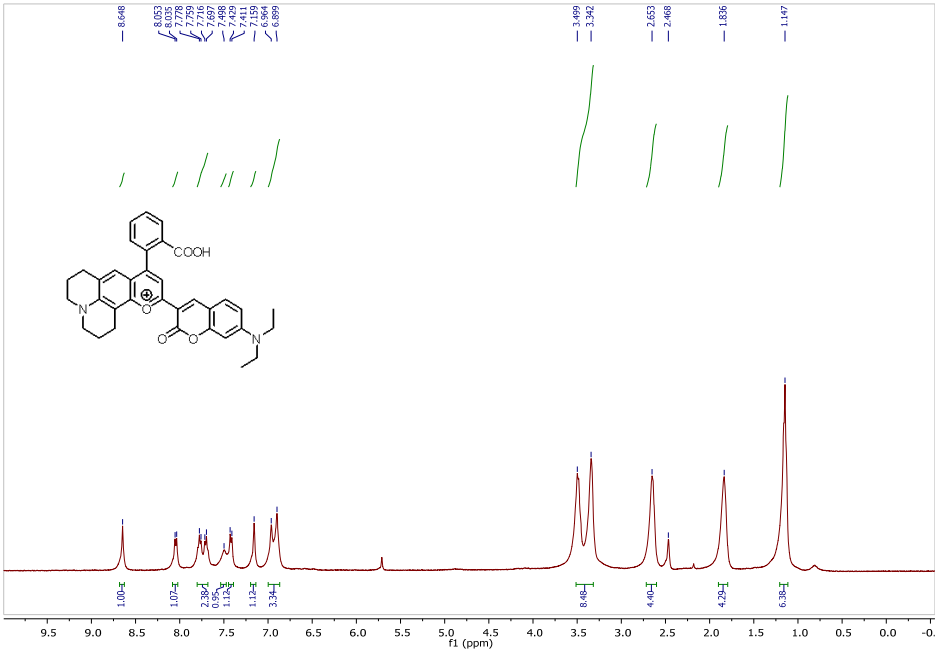

Figure S22. ^{1}H NMR spectrum of compound **8** in DMSO solution.

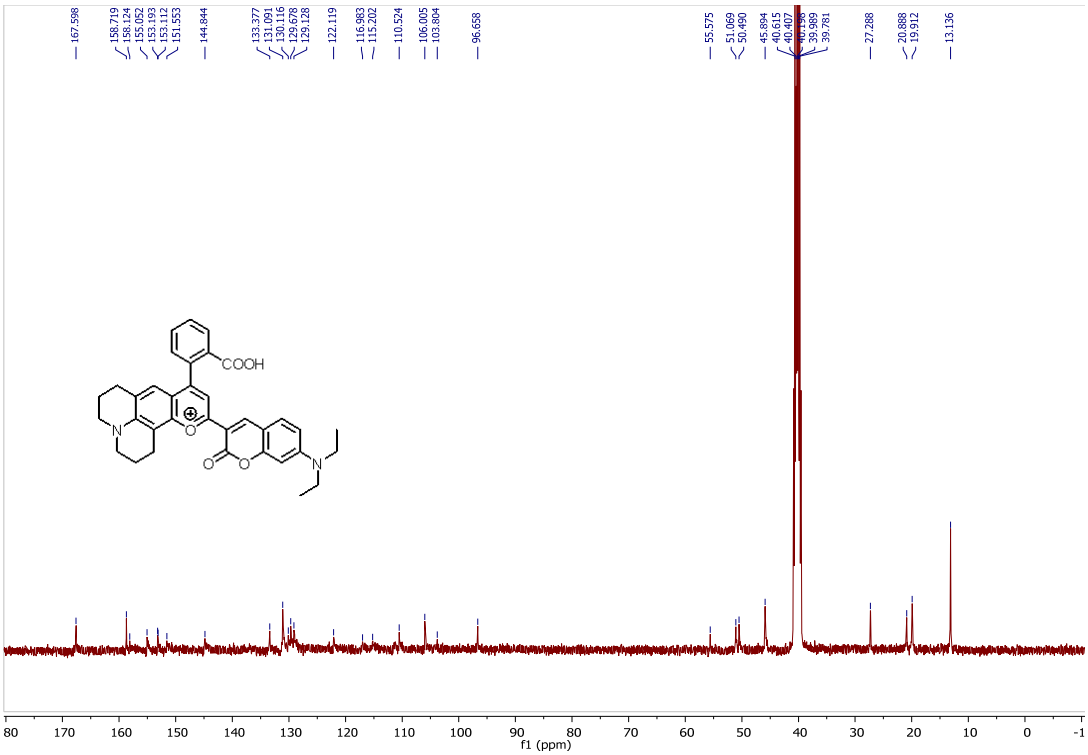

Figure S23. ^{13}C NMR spectrum of compound **8** in DMSO solution.

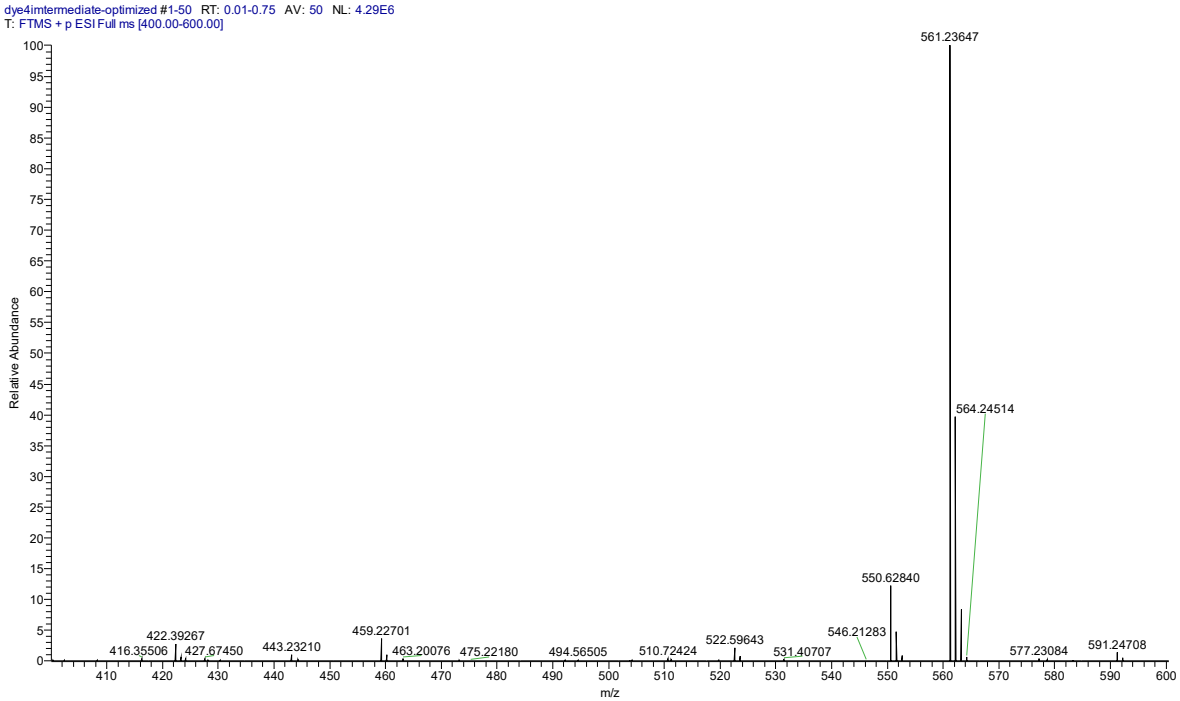

Figure S24. HRMS spectrum of compound **8**.

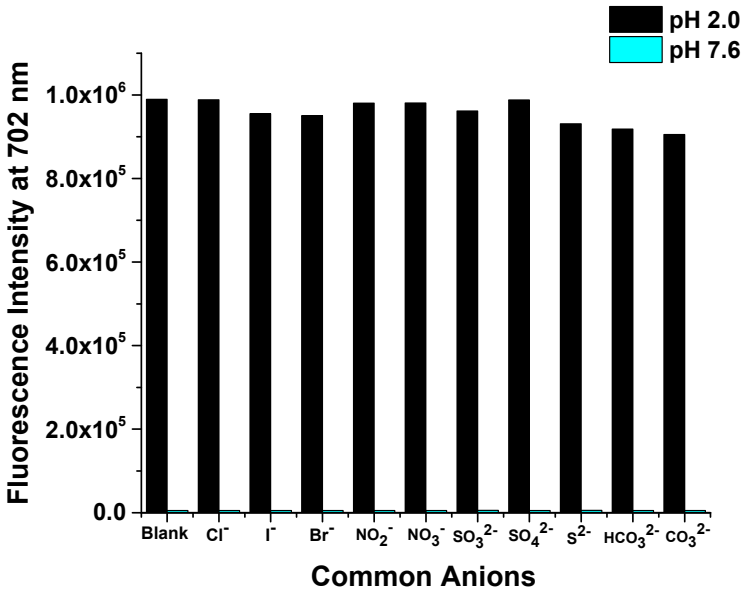

Figure S25. The response of probe **B** to 200 μM common anions in 5 mM citric phosphate buffers with different pH values containing 40% ethanol

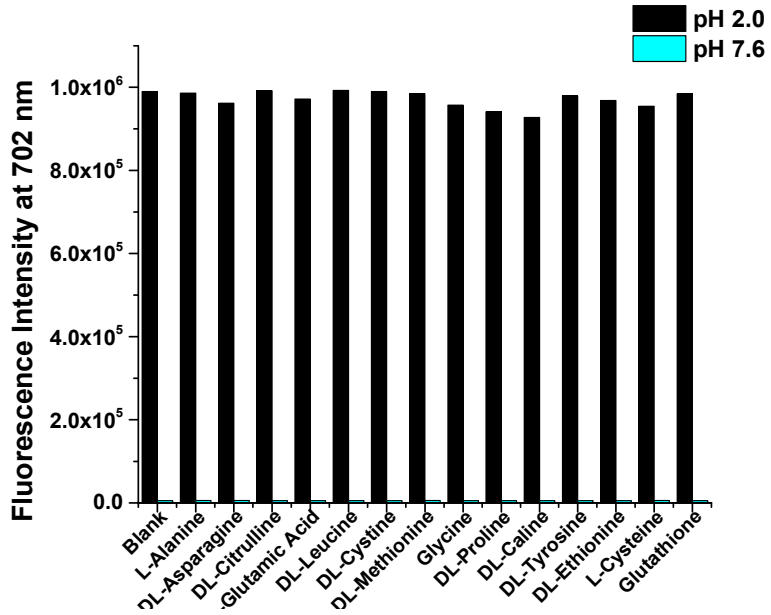

Figure S26. The fluorescence responses of probe **B** to 50 μM amino acids and biothiols in 5 mM citric phosphate buffers with different pH values containing 40% ethanol

Probe A in basic condition

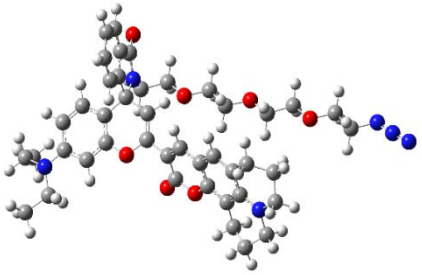

Probe A in acidic condition

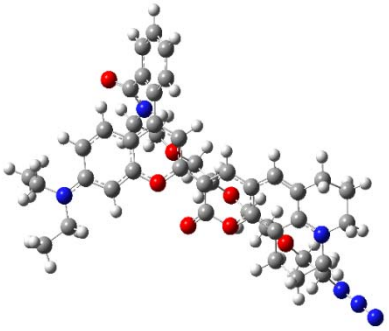

HOMO of probe A in basic condition

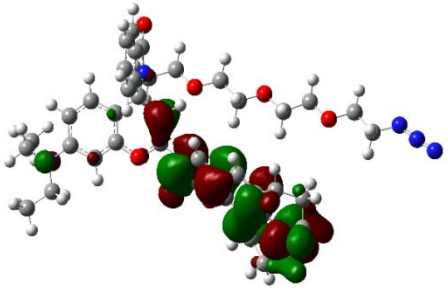

HOMO of probe A in acidic condition

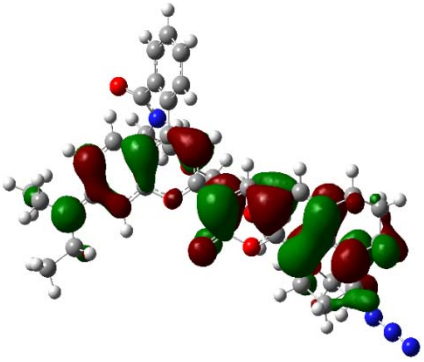

LUMO of probe A in basic condition

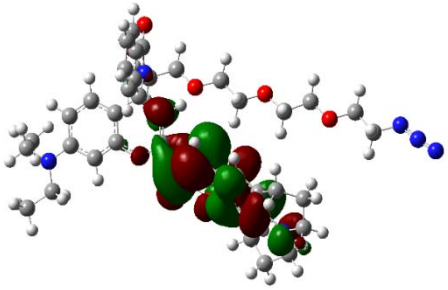

LUMO of probe A in acidic condition

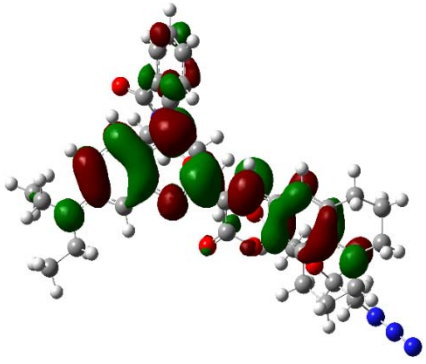

Figure S27: Optimized structures of the protonated and deprotonated forms of fluorescent probe A , with atoms colored as follows carbon is grey, hydrogen is white, nitrogen is blue and oxygen is red. Visualizations of their HOMO and LUMO orbitals are colored by wavefunction in either red or green.

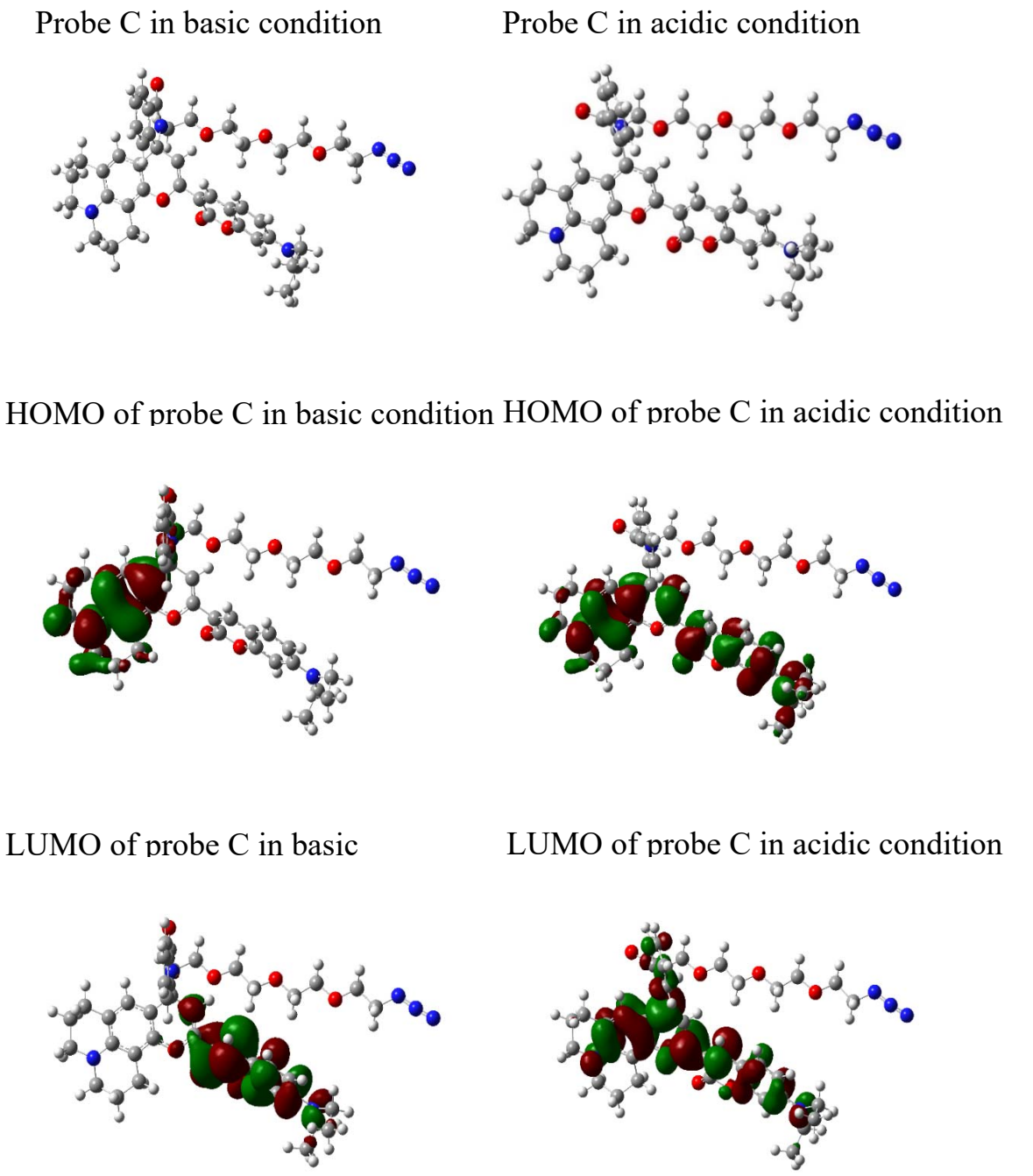

Figure S28: Optimized structures of protonated (right) and deprotonated (left) forms of fluorescent probe C, with atoms colored as follows: carbon -grey, hydrogen - white, nitrogen -blue and oxygen - red. Visualizations of their HOMO and LUMO orbitals are colored by wavefunction in either red or green.

Probe	HOMO Energy (eV)	LUMO Energy (eV)	HOMO-LUMO Energy difference (eV)
A Deprotonated	-0.1882	-0.0608	0.1274
A Protonated	**-0.2021**	**-0.1141**	**0.0880**
B Deprotonated	-0.1941	-0.0645	0.1296
B Protonated	**-0.2081**	**-0.1160**	**0.0922**
C Deprotonated	-0.1810	-0.0634	0.1176
C Protonated	**-0.2036**	**-0.1119**	**0.0917**

Table 1: The calculated HOMO and LUMO energy as well as HOMO-LUMO energy differences of the fluorescent probes **A**, **B** and **C** in both opened (protonated) and closed (deprotonated) spirolactam ring forms.

Probe	Excitation Energy Wavelength (nm)	Oscillator Strength
A Deprotonated	392.2	0.6798
A Protonated	**578.3**	**1.1863**
B Deprotonated	397.8	0.0415
B Protonated	**558.3**	**1.1952**
C Deprotonated	444.8	0.0102
C Protonated	**566.3**	**1.0661**

Table 2: Calculated excitation energy and oscillator strengths for the fluorescent probes **A**, **B** and **C** in both opened (protonated) and closed (deprotonated) spirolactam ring forms.

Compound	HOMO Energy (eV)	LUMO Energy (eV)	HOMO-LUMO Gap Energy (eV)
D Deprotonated	-0.1881	-0.0608	0.1273
D Protonated	**-0.2023**	**-0.1142**	**0.0881**
E Deprotonated	-0.1944	-0.0646	0.1298
E Protonated	**-0.2081**	**-0.1159**	**0.0922**

Table 3: The calculated HOMO and LUMO energy as well as HOMO-LUMO gap energies of fluorescent probes D and E in both their opened (protonated) and closed (deprotonated) spirolactam forms.

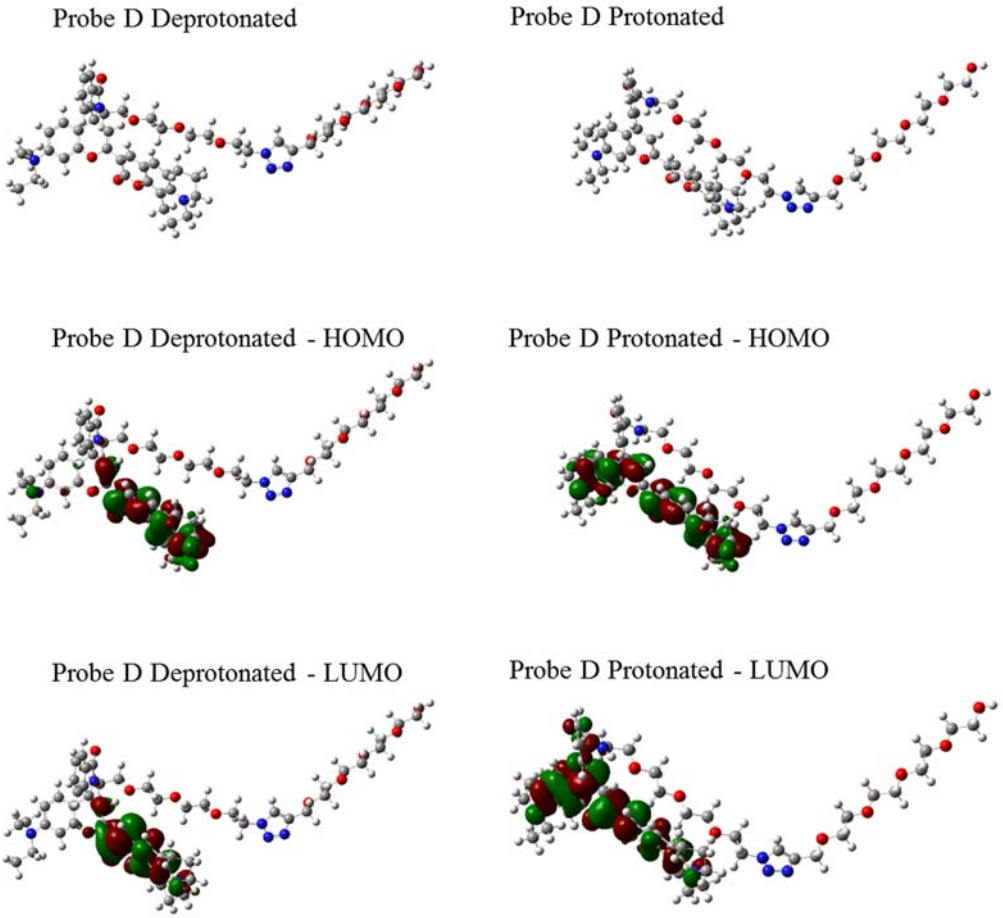

Figure S29: The optimized structures of the closed (deprotonated) and opened (protonated) spirolactam forms of fluorescent probe **D**, with atoms colored as follows carbon is grey, hydrogen is white, nitrogen is blue and oxygen is red. Visualizations of their HOMO and LUMO orbitals are colored by wavefunction in either red or green.

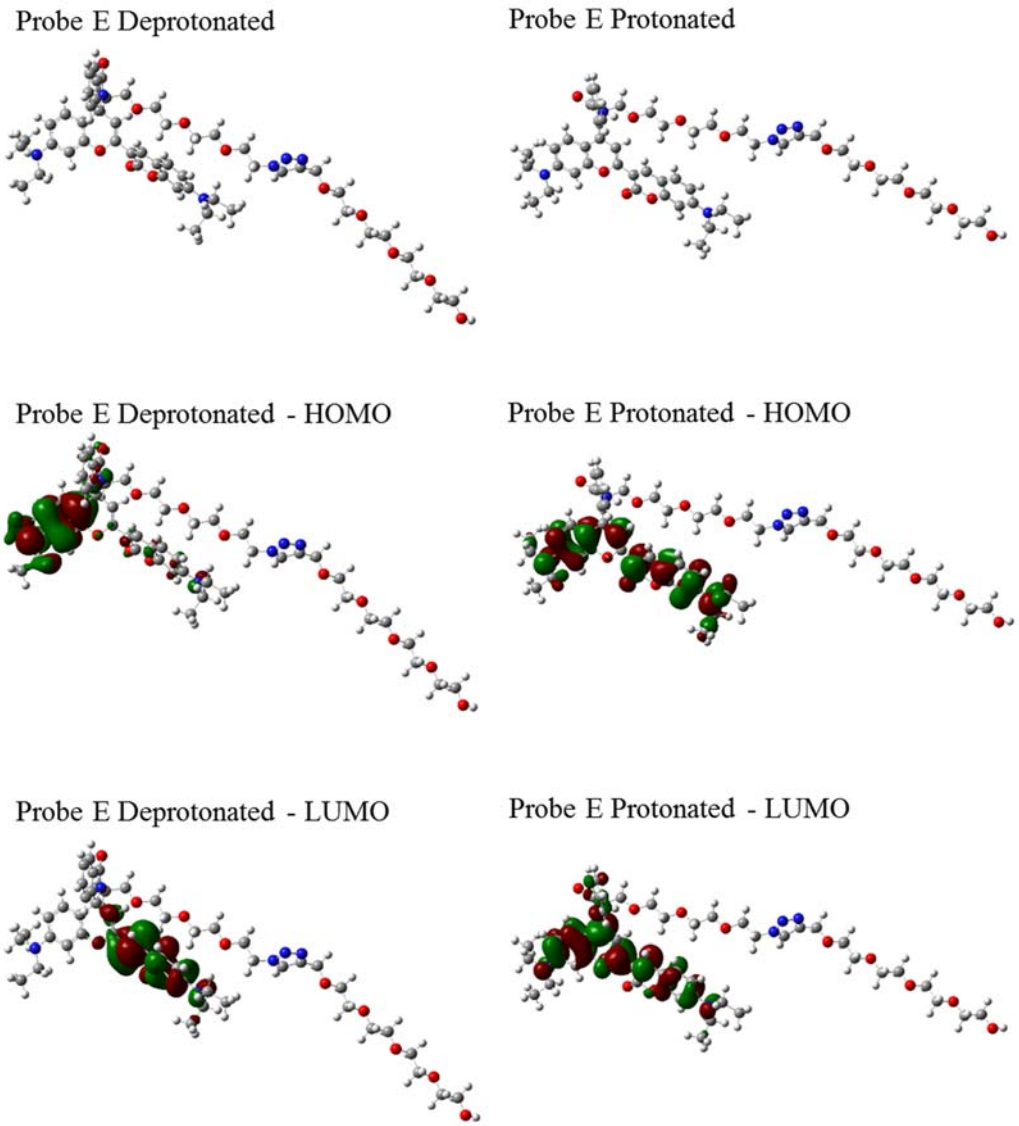

Figure S30: The optimized structures of the closed (deprotonated) and opened (protonated) spirolactam forms of fluorescent probe **E**, with atoms colored as follows carbon is grey, hydrogen is white, nitrogen is blue and oxygen is red. Visualizations of their HOMO and LUMO orbitals are colored by wavefunction in either red or green.

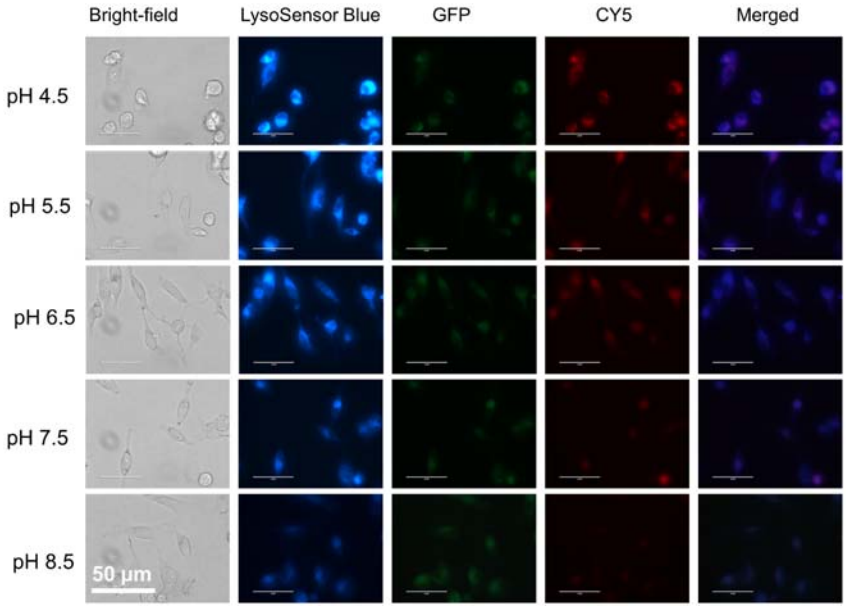

Figure S31: Fluorescence images of MDA-MB231 cells incubated with fluorescent probe **B**. MDA-MB231 cells were incubated with 5 µM probe **B** at different pH values ranging from pH 4.5 to 8.5 in presence of LysoSensor blue DND-167 (2 µM) and nigericin. Images were acquired using the inverted fluorescence microscope (AMF-4306, EVOSfl, AMG) at 60X magnification.

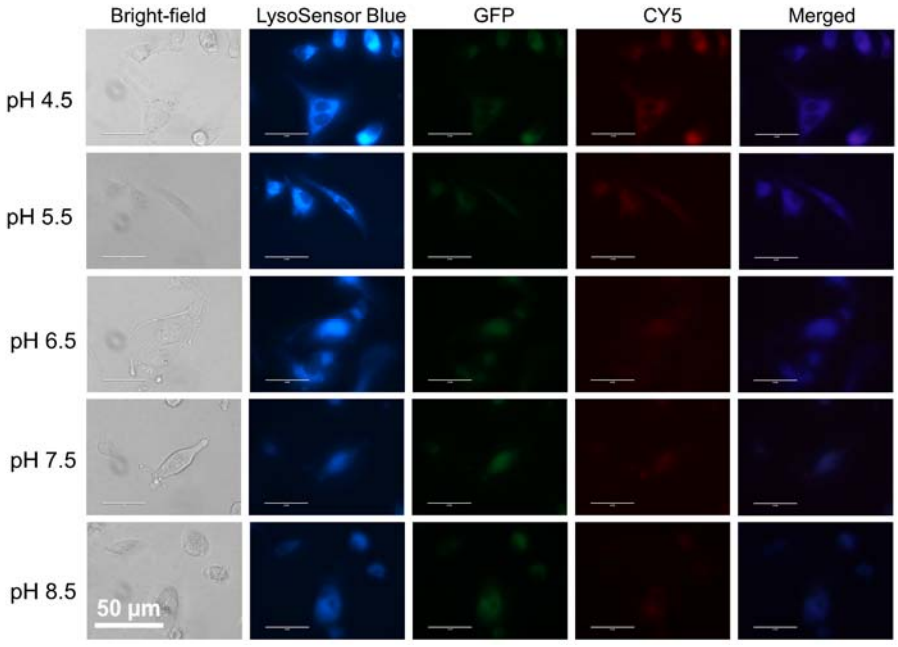

Figure S32: Fluorescence images of HUVEC-C cells incubated with fluorescent probe **B**. HUVEC-C cells were incubated with 5 µM probe **B** at different pH values ranging from pH 4.5 to 8.5 in presence of LysoSensor blue DND-167 (2 µM) and nigericin. Images were acquired using the inverted fluorescence microscope (AMF-4306, EVOSfl, AMG) at 60X magnification.

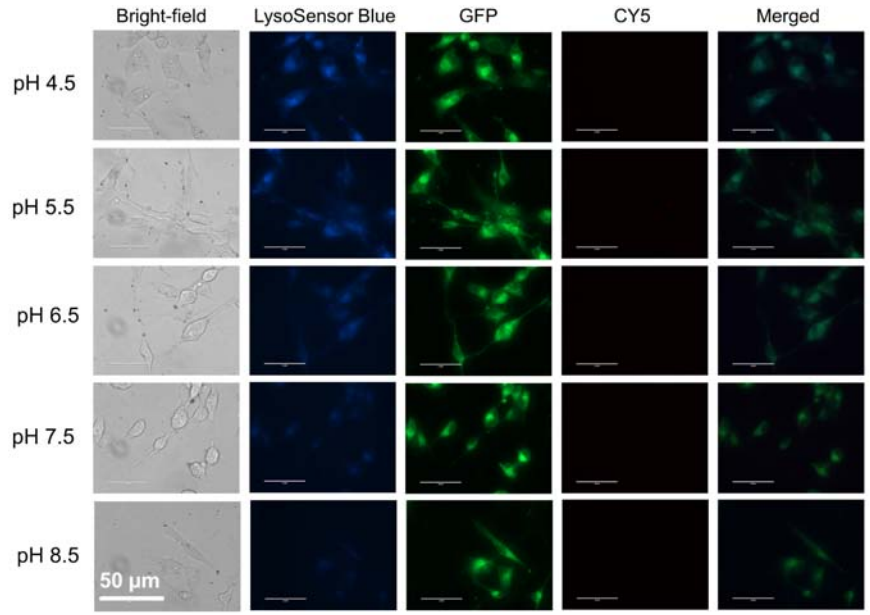

Figure S33: Fluorescence images of MDA-MB231 cells incubated with fluorescent probe **A**. MDA-MB231 cells were incubated with 10 µM probe **A** at different pH values ranging from pH 4.5 to 8.5 in presence of LysoSensor blue DND-167 (2 µM) and nigericin. Images were acquired using the inverted fluorescence microscope (AMF-4306, EVOSfl, AMG) at 60X magnification.

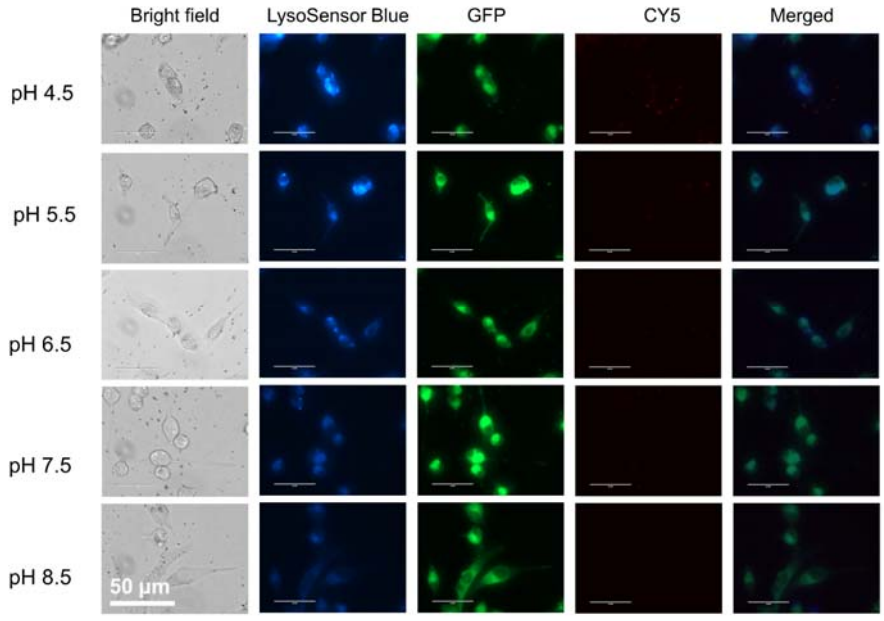

Figure S34: Fluorescence images of MDA-MB231 cells incubated with fluorescent probe **A**. MDA-MB231 cells were incubated with 20 µM probe **A** at different pH values ranging from pH 4.5 to 8.5 in presence of LysoSensor blue DND-167 (2 µM) and nigericin. Images were acquired using the inverted fluorescence microscope (AMF-4306, EVOSfl, AMG) at 60X magnification.

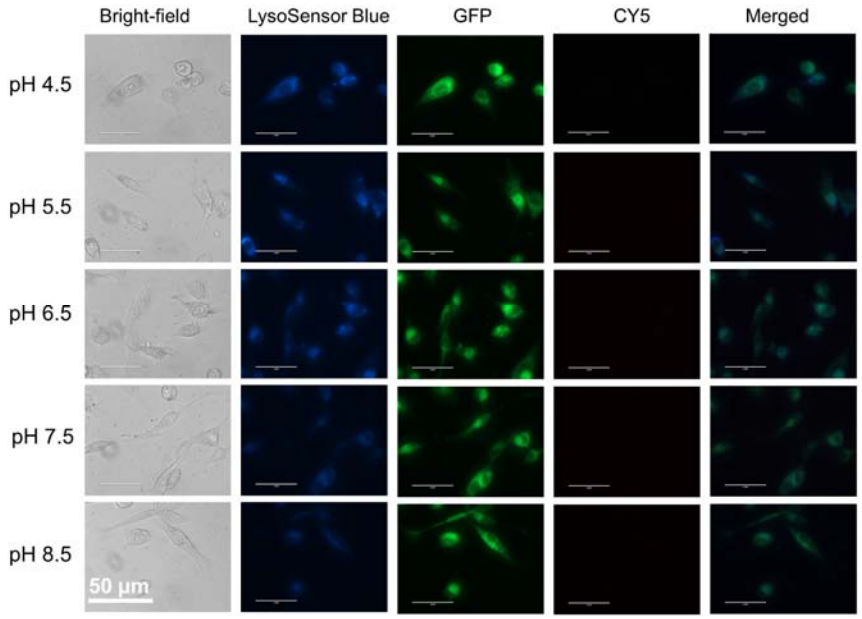

Figure S35: Fluorescence images of MDA-MB231 cells incubated with fluorescent probe **C**. MDA-MB231 cells were incubated with 10 µM probe **C** at different pH values ranging from pH 4.5 to 8.5 in presence of LysoSensor blue DND-167 (2 µM) and nigericin. Images were acquired using the inverted fluorescence microscope (AMF-4306, EVOSfl, AMG) at 60X magnification.

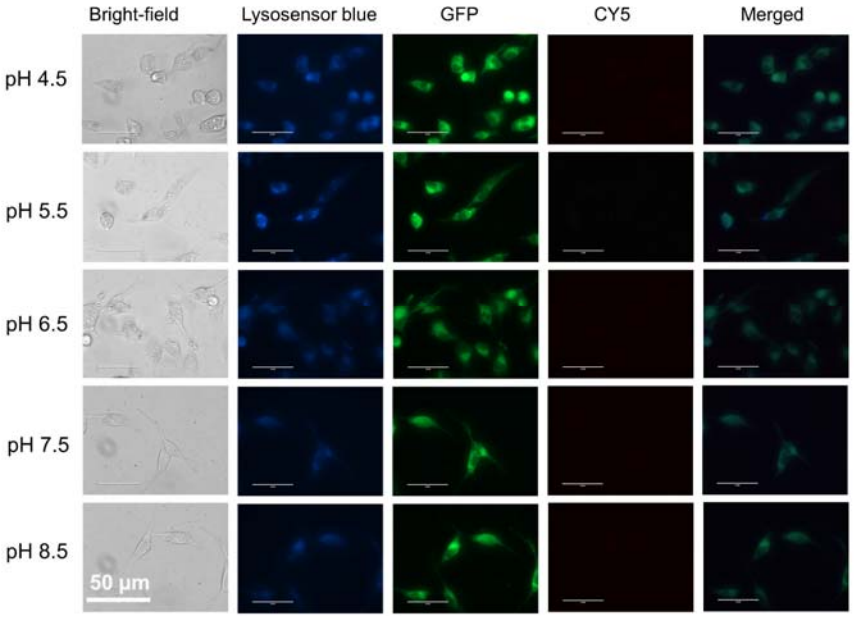

Figure S36: Fluorescence images of MDA-MB231 cells incubated with fluorescent probe **D**. MDA-MB231 cells were incubated with 5 µM probe **D** at different pH values ranging from pH 4.5 to 8.5 in presence of LysoSensor blue DND-167 (2 µM) and nigericin. Images were acquired using the inverted fluorescence microscope (AMF-4306, EVOSfl, AMG) at 60X magnification.

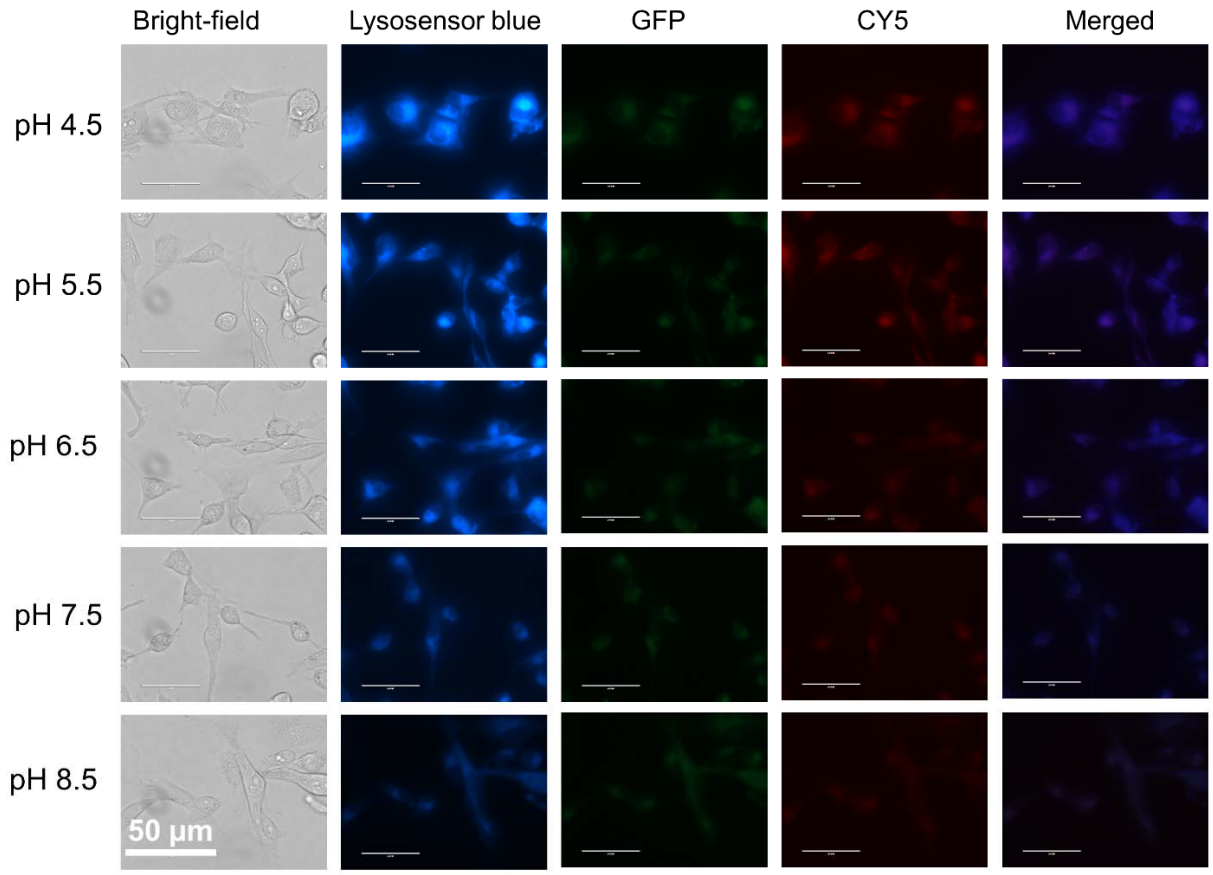

Figure S37: Fluorescence images of MDA-MB231 cells incubated with fluorescent probe **E**. MDA-MB231 cells were incubated with 5 µM probe **E** at different pH values ranging from pH 4.5 to 8.5 in presence of LysoSensor blue DND-167 (2 µM) and nigericin. Images were acquired using the inverted fluorescence microscope (AMF-4306, EVOSfl, AMG) at 60X magnification.

(a)

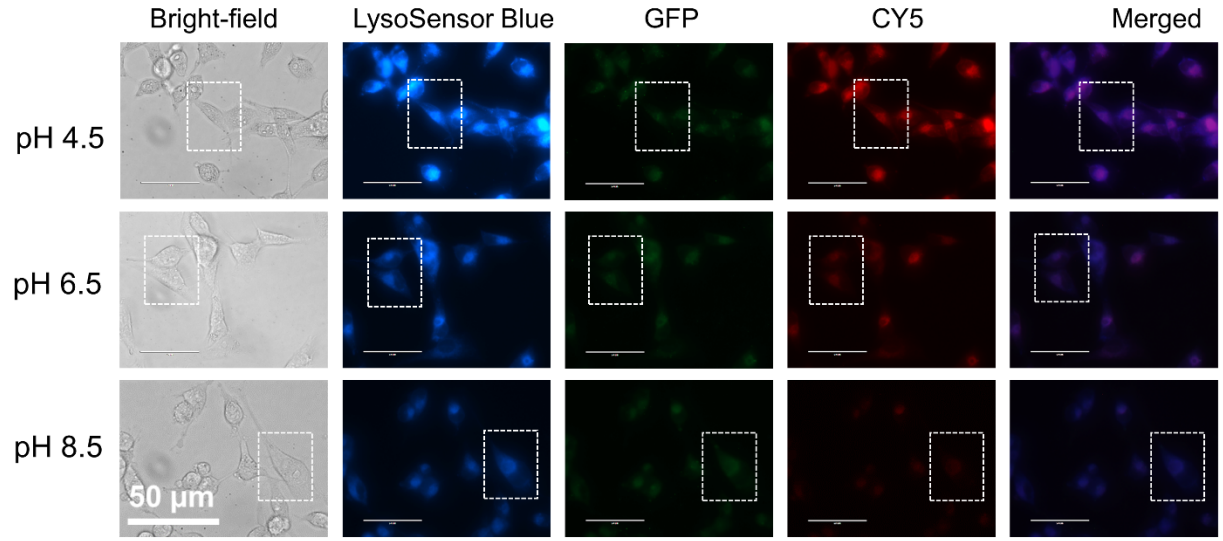

(b)

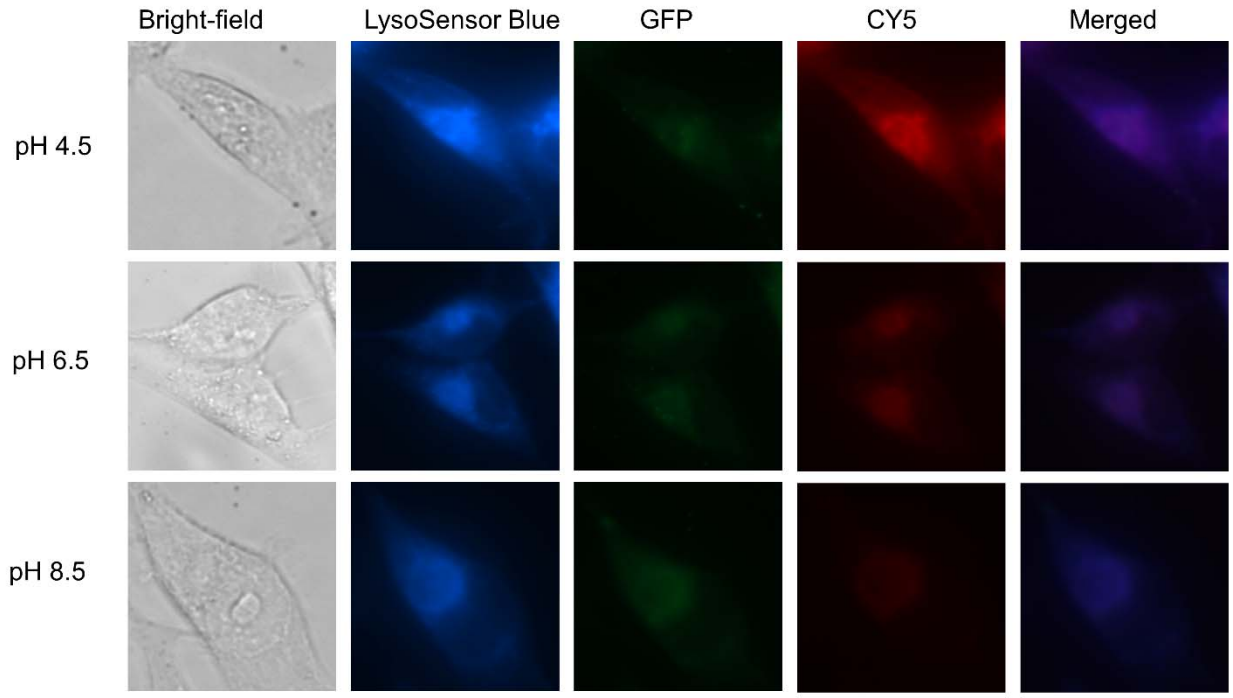

Figure S38: Fluorescence images of MDA-MB231 cells incubated with fluorescent probe **B**. (a) MDA-MB231 cells were incubated with 10 µM probe **B** at different pH values ranging from pH 4.5 to 8.5 in presence of LysoSensor blue DND-167 (2 µM) and nigericin. Images were acquired using the inverted fluorescence microscope (AMF-4306, EVOSfl, AMG) at 60X magnification. (b) Enlarged fluorescence images of MDA-MB231 cells from figure (a).

(a)

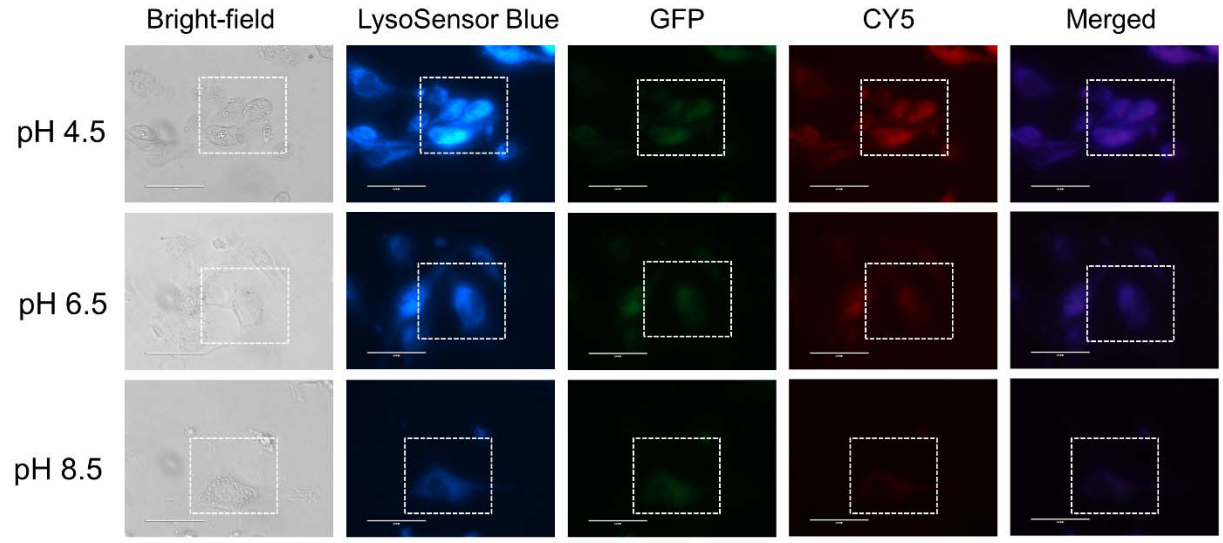

(b)

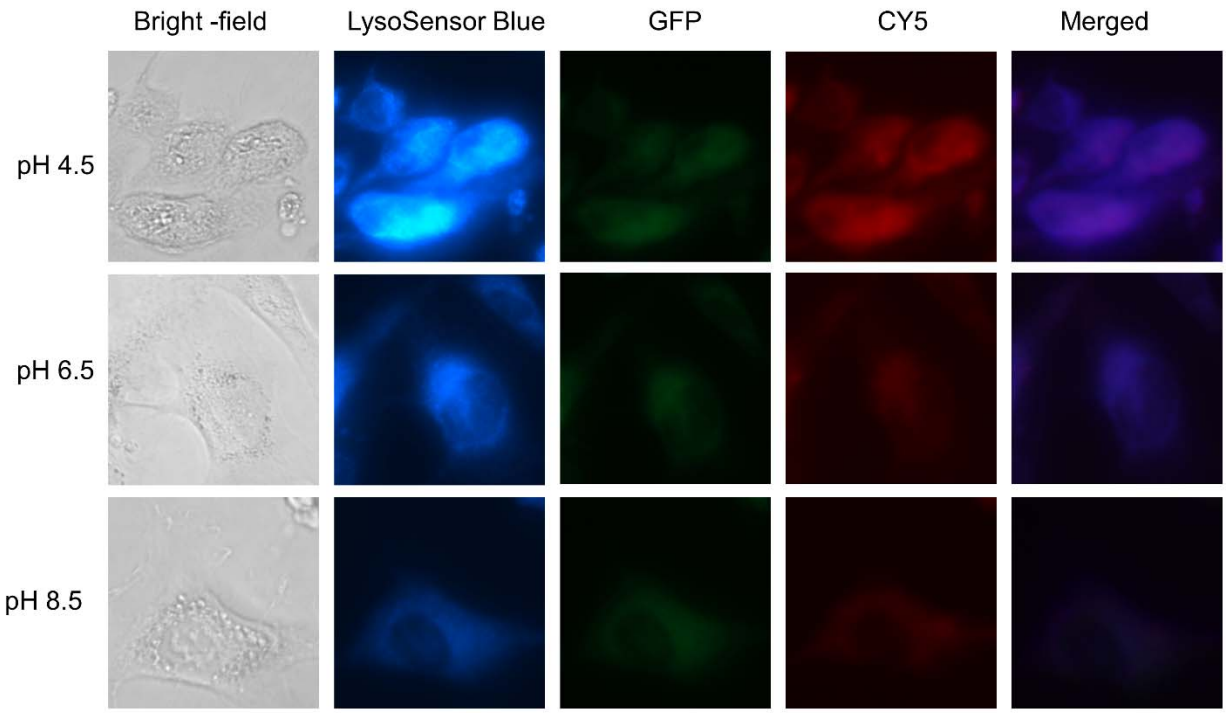

Figure S39: Enlarged fluorescence images of HUVEC-C cells incubated with 10 µM fluorescent probe **B**. (a) HUVEC-C cells were incubated with 10 µM probe **B** at different pH values ranging from pH 4.5 to 8.5 in presence of LysoSensor blue DND-167 (2 µM) and nigericin. Images were acquired using the inverted fluorescence microscope (AMF-4306, EVOSfl, AMG) at 60X magnification. (b) Enlarged fluorescence images of HUVEC-C cells from figure (a).

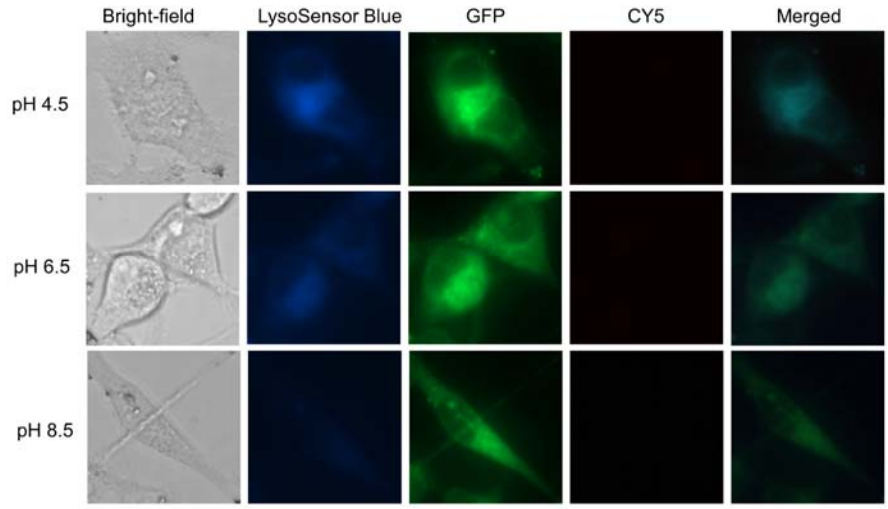

Figure S40: Enlarged fluorescence images of MDA-MB231 cells incubated with 10 µM fluorescent probe **A** . MDA-MB231 cells were incubated with 10 µM probe **A** at different pH values ranging from pH 4.5 to 8.5 in presence of LysoSensor blue DND-167 (2 µM) and nigericin. Images were acquired using the inverted fluorescence microscope (AMF-4306, EVOSfl, AMG) at 60X magnification. The images taken at 60X were enlarged to observe the co-localization of probe with LysoSensor blue DND-167.

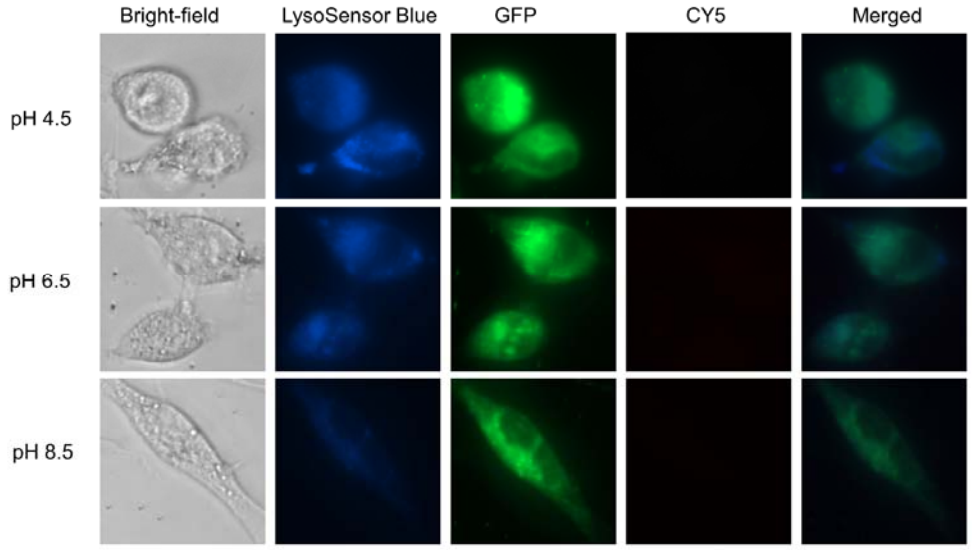

Figure S41: Enlarged fluorescence images of MDA-MB231 cells incubated with 10 µM fluorescent probe **C**. MDA-MB231 cells were incubated with 10 µM probe **C** at different pH values ranging from pH 4.5 to 8.5 in presence of LysoSensor blue DND-167 (2 µM) and nigericin. Images were acquired using the inverted fluorescence microscope (AMF-4306, EVOSfl, AMG) at 60X magnification. The images taken at 60X were enlarged to observe the co-localization of probe with LysoSensor blue DND-167.

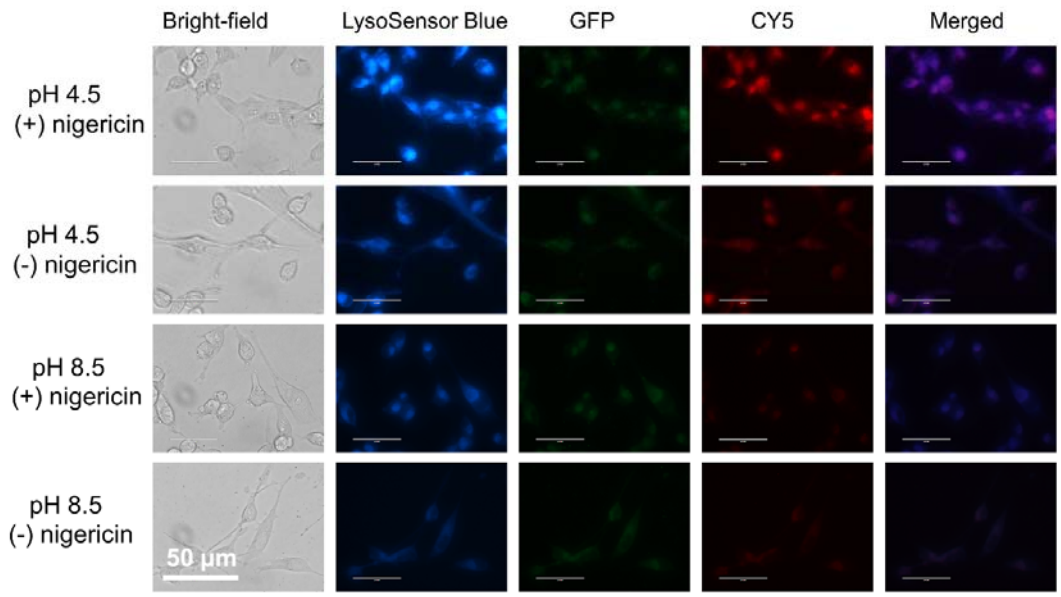

Figure S42: Fluorescence images of MDA-MB231 cells incubated with fluorescent probe **B**. MDA-MB231 cells were incubated with 10 µM probe **B** at pH values 4.5 and 8.5 in presence of LysoSensor blue DND-167 (2 µM) with and without nigericin. Images were acquired using the inverted fluorescence microscope (AMF-4306, EVOSfl, AMG) at 60X magnification.

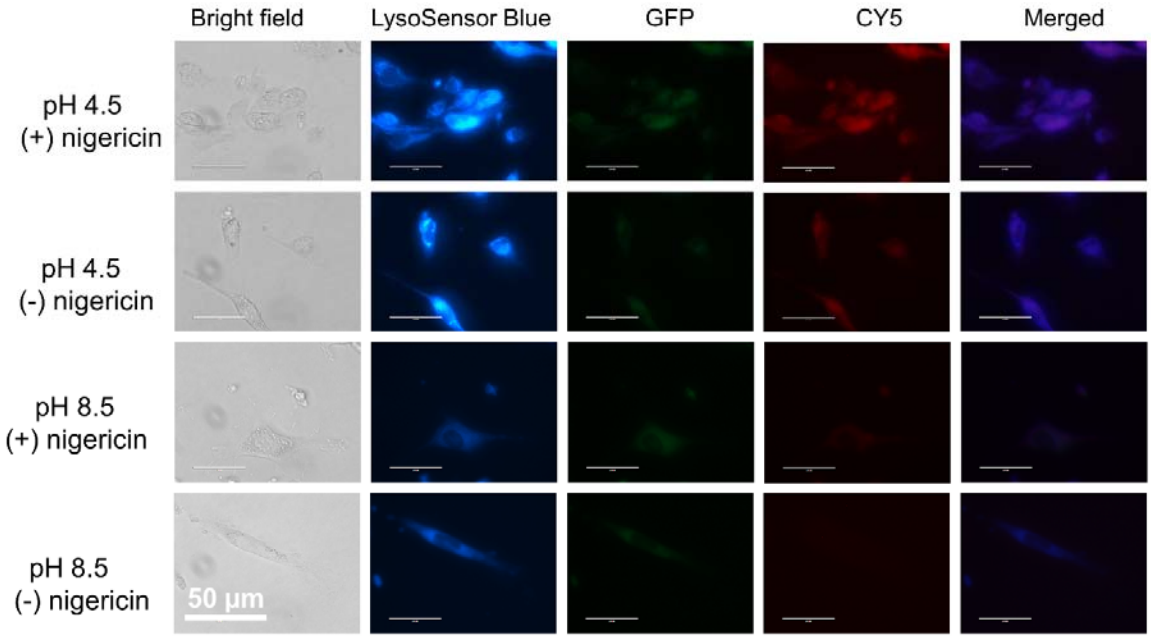

Figure S43: Fluorescence images of HUVEC-C cells incubated with fluorescent probe **B**. HUVEC-C cells were incubated with 10 µM probe **B** at pH values 4.5 and 8.5 in presence of LysoSensor blue DND-167 (2 µM) with and without nigericin. Images were acquired using the inverted fluorescence microscope (AMF-4306, EVOSfl, AMG) at 60X magnification.

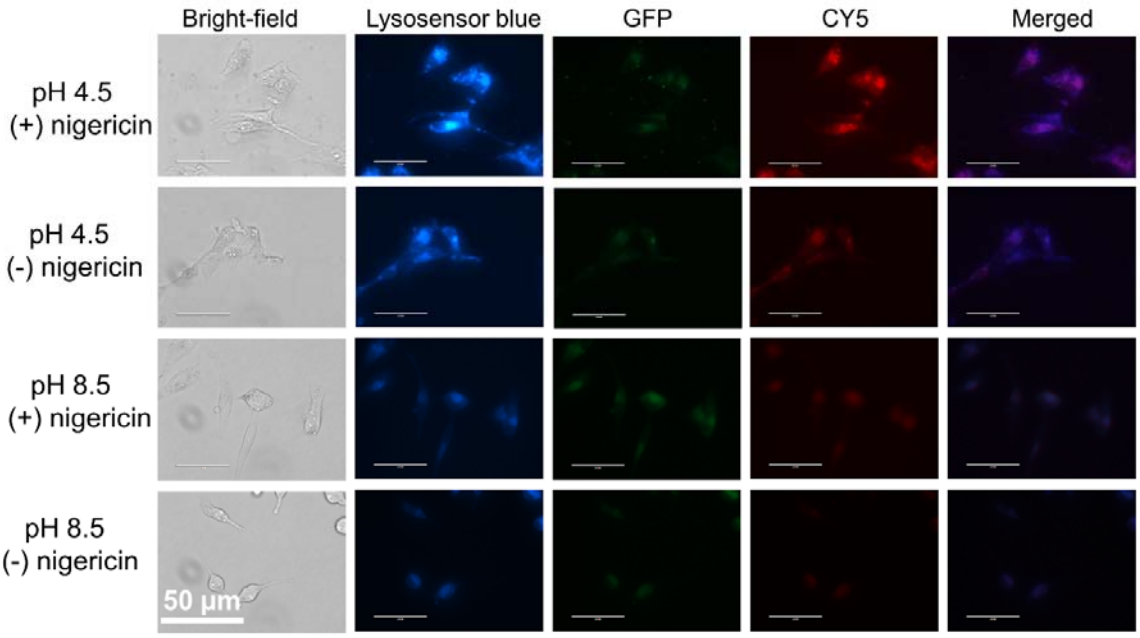

Figure S44: Fluorescence images of MDA-MB231 cells incubated with fluorescent probe **E**. MDA-MB231 cells were incubated with 10 µM probe **E** at pH values 4.5 and 8.5 in presence of LysoSensor blue DND-167 (2 µM) with and without nigericin. Images were acquired using the inverted fluorescence microscope (AMF-4306, EVOSfl, AMG) at 60X magnification.

References

1. Albert M. Brouwer, Standards for photoluminescence quantum yield measurements in solution (IUPAC Technical Report), *Pure Appl. Chem.*, Vol. 83, No. 12, pp. 2213–2228, 2011. doi:10.1351/PAC-REP-10-09-31
2. Yuan, Lin, et al. "A unique class of near-infrared functional fluorescent dyes with carboxylic-acid-modulated fluorescence ON/OFF switching: rational design, synthesis, optical properties, theoretical calculations, and applications for fluorescence imaging in living animals." *J. Am. Chem. Soc.*, 134.2 (2012): 1200-1211.
3. Cielen, E.; Tahri, A.; Heyen, K. V.; Hoornaert, G. J.; De Schryver, F. C.; Boens, N., Synthesis and Spectroscopic Characterisation of Fluorescent Indicators for Na^+ and K^+. *J. Chem. Soc. Perkin Trans.2*, 0(1998), 1573-1580.